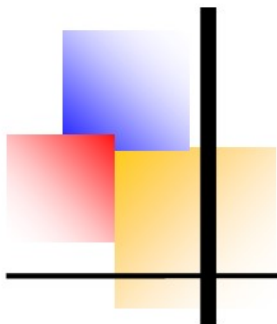# Appendix A.5:

Modeling Fine Particulate Matter Emissions from the PBF Martinez Refinery: An Air Quality Analysis (Interim DRAFT Report – Version 2)

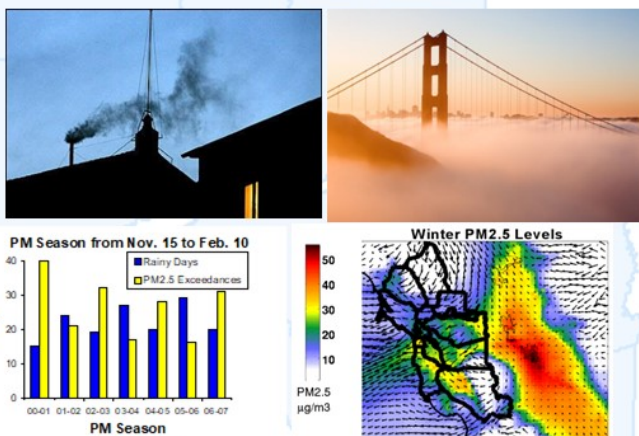Changes since version 1: Appendix A.5 reordered within Appendix A.

Modeling Fine Particulate Matter Emissions From the PBF Martinez Refinery: An Air Quality Analysis (Interim DRAFT Report – Version 2)

March 2021

Prepared by Modeling and Analysis Section Staff:

Bonyoung Koo, Senior Atmospheric Modeler
Yiqin Jia, Atmospheric Modeler
James Cordova, Air Quality Meteorologist
Yuanyuan Fang, Statistician
Stephen Reid, Senior Advanced Projects Advisor
Jeff Matsuoka, Research Analyst

Contributors:

Tan Minh Dinh, Air Quality Engineer
Anne Werth, Supervising Air Quality Engineer
Andrea Baird, Technical Editor
Song Bai, Emissions and Community Exposure Assessment Manager
Saffet Tanrikulu, Air Quality Modeling and Analysis Manager

Table of Contents

Executive Summary

Introduction

Staff at the Bay Area Air Quality Management District (Air District or BAAQMD) are in the process of estimating contributions of directly emitted fine particulate matter (PM$_{2.5}$) from major industrial facilities in the Bay Area to ambient PM$_{2.5}$ levels. This report presents results from modeling analyses for the PBF refinery in Martinez, California. Results for the Chevron refinery have been previously reported, and those for other facilities are forthcoming. Analyses of human exposure to estimated PM$_{2.5}$ levels for each facility will be reported as they become available. The purpose of this effort is to provide technical information to supplement the Air District's rule development efforts and to support the Air District's assessments related to the implementation of Assembly Bill 617 (AB 617).

The California Puff (CALPUFF) model will be used for estimating ambient PM$_{2.5}$ levels contributed by major facilities. Emissions from each major facility will be separately simulated using CALPUFF. Two sets of receptor domains will be established. One will cover the entire Bay Area at 1-km grid resolution, and the other will cover areas with simulated PM$_{2.5}$ concentrations above 0.1 µg/m^3 at 100-m grid resolution.

CALPUFF will be applied for three years (2016, 2017, and 2018) using year-specific meteorology and the same base-year (2018) emission estimates. Average results from the three annual simulations will be used for analyses to minimize the impact of year-to-year variability in meteorology on ambient PM$_{2.5}$ levels.

CALPUFF requires an emissions input file that includes detailed information for each modeled source, including source ID number, location coordinates, base elevation, stack height, stack diameter, gas exit velocity, gas exit temperature, and emission rate. There were 63 release points identified for the PM$_{2.5}$ emissions at the PBF refinery and an estimated total (in 2018) of 463 tons of PM$_{2.5}$ emitted annually. The single largest source, the fluid catalytic cracking unit (FCCU), is responsible for about two-thirds (65%) of the annual PM$_{2.5}$ emissions.

It should be noted that all emissions and stack parameter data represent the best available information at the time the modeling was conducted. Prior to modeling, quality control (QC) checks were performed on the stack-level data. For example, source locations were plotted and reviewed. In addition, minimum and maximum values for each stack parameter were identified to make sure that all values fell within reasonable bounds.

Meteorological inputs to CALPUFF were prepared using the Weather Research and Forecasting (WRF) model. The WRF model was tested using available options for physics and dynamics, as well as the datasets used to initialize and drive the model. Results of each test were evaluated, and the best-performing set of options was selected for final modeling.

Results

Simulation results are presented for three different emissions scenarios: emissions from (1) all point sources, (2) FCCU only, and (3) FCCU with an assumed wet gas scrubber. Key findings are tabulated, illustrated, and discussed below.

Simulations with Emissions from All Sources

Figure ES.1 shows the three-year (2016–2018) average CALPUFF-simulated $PM_{2.5}$ concentrations for the 100-m receptor domain. Estimated concentrations within the PBF facility fence line and concentrations below 0.1 μg/m^3 are not shown.

CALPUFF estimates concentrations at receptor points located at the center of each 100 x 100 m grid cell. For mapping purposes, each grid cell is color coded based on the concentration value at its center. An interval of 0.5 μg/m^3 was selected for color coding (except for concentrations between 0.1 μg/m^3 and 0.5 μg/m^3).

As can be seen in Figure ES.1a, the lowest concentration bin (0.1 μg/m^3 to 0.5 μg/m^3) extends from Pleasant Hill in the south to Birds Landing in the north and from Pinole Valley in the west to Decker Island in the east. The emissions plume has an elongated shape in the southwesterly and northeasterly directions from Martinez, consistent with predominant winter and summer wind patterns there, respectively.

The area with concentrations above 0.5 μg/m^3 is much smaller than the area covered by the lowest concentration bin, as described above. These higher concentrations are mostly confined to the area around the PBF facility and extend toward the northeast of the facility.

To better visualize the high-concentration areas, a zoomed-in map of the 100-m receptor domain was created (Figure ES.1b). As shown in this figure, an area with concentrations between 0.5 μg/m^3 and 1.0 μg/m^3 extends from the east side of the facility toward Port Chicago, between the southern bank of Suisun Bay and California Highway 4. There is also a small area with concentrations between 0.5 μg/m^3 and 1.0 μg/m^3 to the west of the PBF facility.

Concentrations above 1.0 μg/m^3 primarily lie to the east of the facility over an area that does not overlap residential zones in the region. In addition, a sharp concentration gradient is apparent near the facility fence line. The maximum concentration (3.8 μg/m^3) is located just outside the fence line.

Simulations with FCCU Emissions

CALPUFF was also run with emissions from only the FCCU for two scenarios: one with the baseline FCCU emissions, and the other with reduced FCCU emissions (and altered stack parameters) consistent with the installation of a wet gas scrubber (WGS). The resulting three-year average $PM_{2.5}$ concentrations are shown in Figure ES.2 (FCCU without WGS) and Figure ES.3 (FCCU with WGS installed). Again, concentrations within the facility fence line and below 0.1 µg/m^3 are not shown. An interval of 0.2 µg/m^3 was selected for color coding concentration values at grid cells.
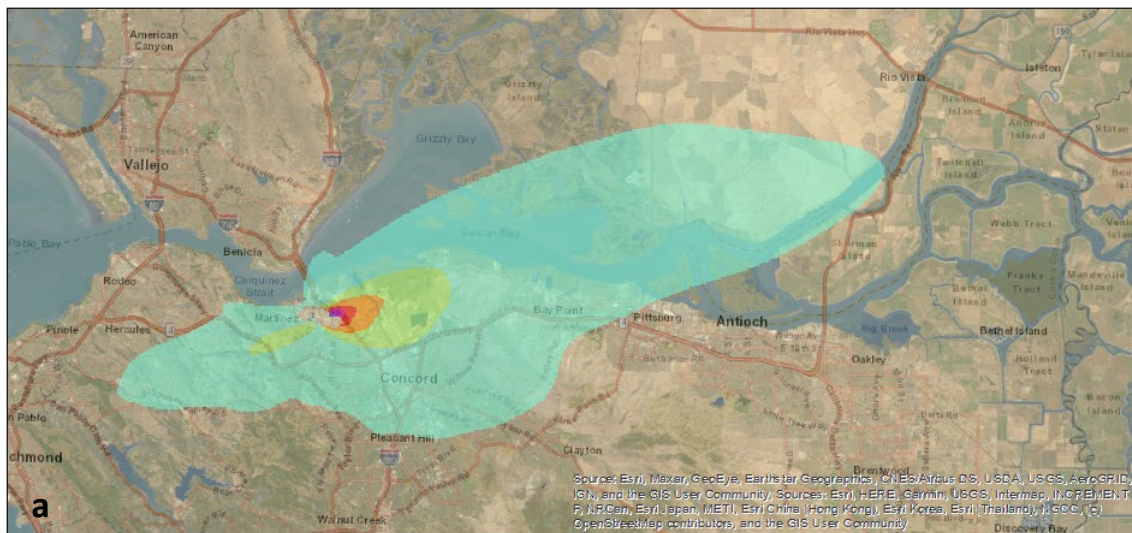
Emissions from this source are mainly transported to the southwest and northeast of the facility, similar to the all-source results, but with smaller impact areas: the number of sampling receptors (100-m grid) with three-year average concentrations above 0.1 µg/m^3 was reduced from 42,741 (all-source simulation) to 21,452 (FCCU-only simulation), i.e., a 50% reduction. The maximum three-year average concentration from this source is 2.0 µg/m^3, or about 53% of the maximum concentration from the all-source simulation. This is somewhat lower than the contribution of the FCCU to the total $PM_{2.5}$ emissions from the facility (65%).

Installation of a WGS further reduces the number of receptors with three-year average concentrations above 0.1 µg/m^3 to 1,078 (a 95% reduction from the baseline FCCU emission scenario) and reduces the maximum three-year average concentration to 0.46 µg/m^3 (22% of the maximum concentration from the baseline FCCU emission scenario). This reduction in the maximum concentration is consistent with the emission reduction by a WGS (78%), as the maximum concentration occurs close to the source location.

Table ES.1 shows the key findings of simulations with the three sets of emissions.

Table ES.1: Key findings of simulations with emissions from all point sources, FCCU only, and FCCU with assumed WGS. Results shown are for the 100-m receptor domain.

	Annual $PM_{2.5}$ emissions (tons/year)	Maximum simulated concentrations (µg/m^3)	Number of sampling receptors with concentrations above 0.1 µg/m^3
All point sources	463.20	3.8	42,741
FCCU only	299.61	2.0	21,452
FCCU with assumed WGS	65.91	0.46	1,078
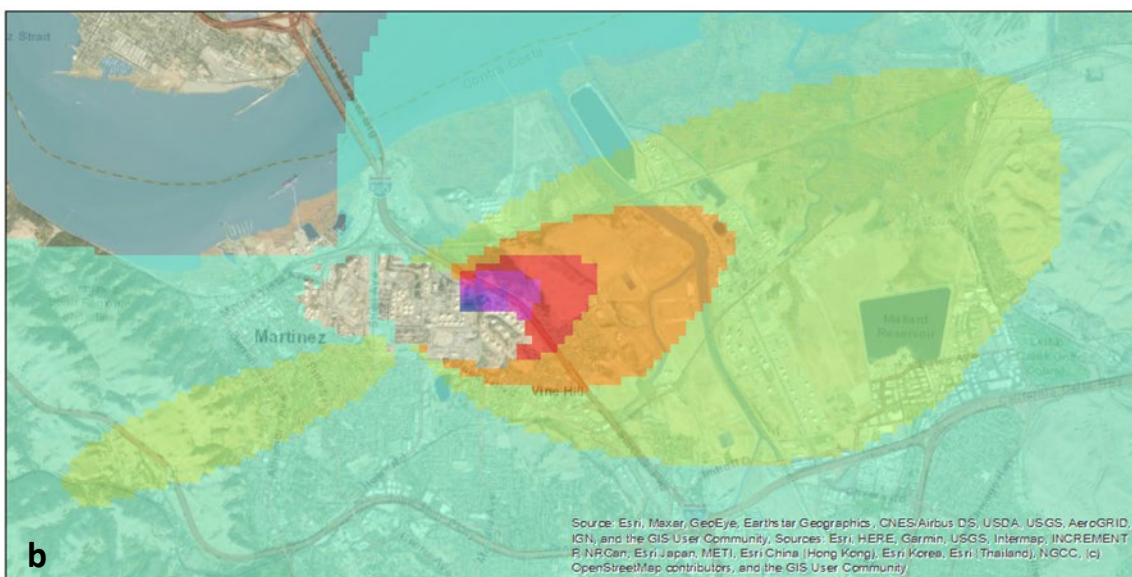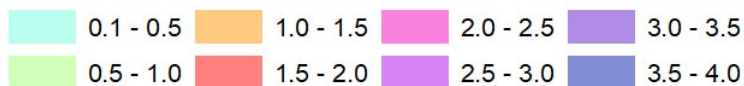
Figure ES.1: Three-year (2016–2018) average CALPUFF-simulated $PM_{2.5}$ concentrations for (a) the 100-m receptor domain, and (b) a zoomed-in area of high concentrations. Emissions from all PBF point sources are included in this simulation. Concentrations inside the PBF fence line and that are below 0.1 μg/m^3 are not shown.
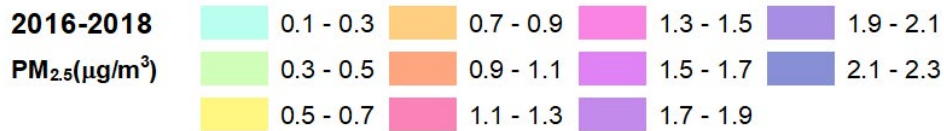
Figure ES.2: Three-year (2016–2018) average CALPUFF-simulated $PM_{2.5}$ concentrations for: (a) the 100-m receptor domain, and (b) a zoomed-in area of high concentrations. Emissions from the FCCU only (without a WGS) are included in these simulations. Concentrations inside the PBF fence line and that are below 0.1 µg/m^3 are not shown.

PBF FCCU WGS

2016-2018		0.1 - 0.3		0.7 - 0.9		1.3 - 1.5		1.9 - 2.1
$PM_{2.5} (\mu g/m^3)$		0.3 - 0.5		0.9 - 1.1		1.5 - 1.7		2.1 - 2.3
		0.5 - 0.7		1.1 - 1.3		1.7 - 1.9		

PBF FCCU WGS

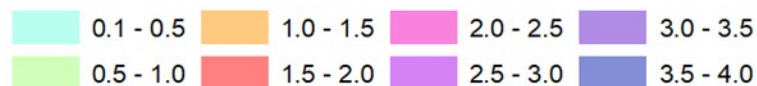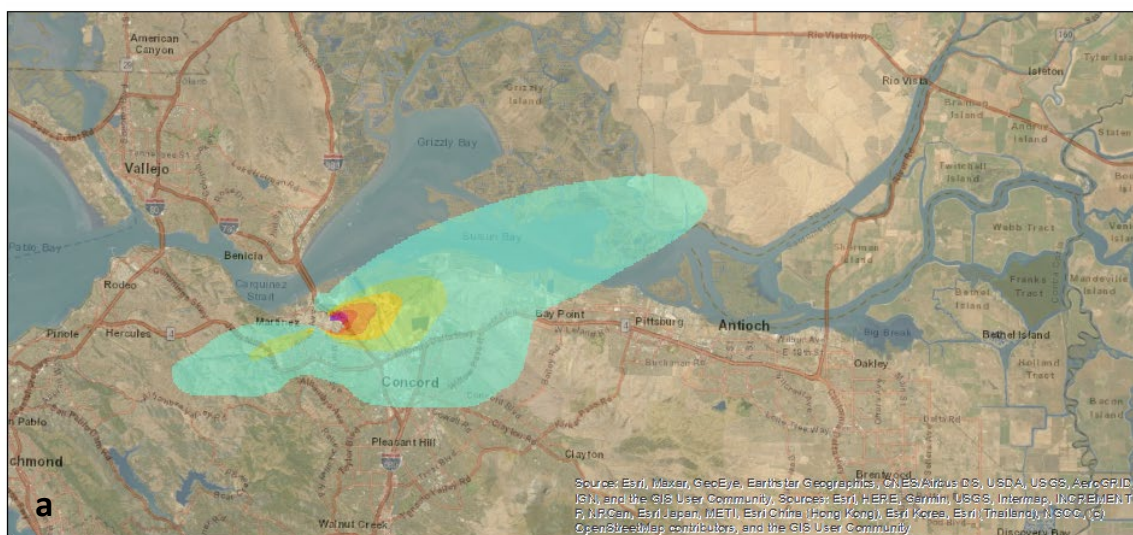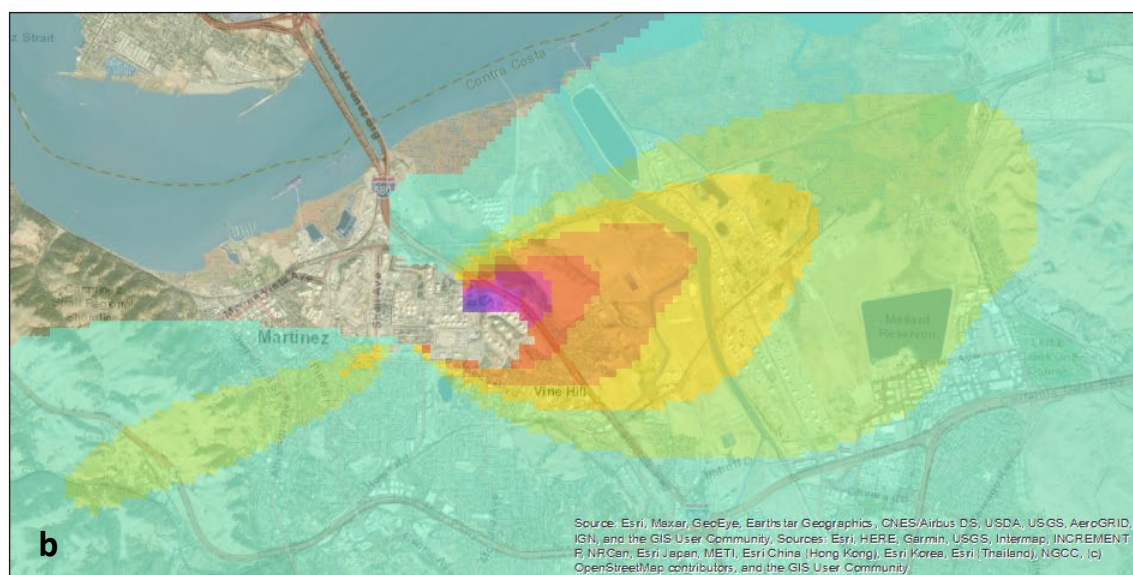| 2016-2018		0.1 - 0.3		0.7 - 0.9		1.3 - 1.5		1.9 - 2.1
$PM_{2.5} (\mu g/m^3)$		0.3 - 0.5		0.9 - 1.1		1.5 - 1.7		2.1 - 2.3
		0.5 - 0.7		1.1 - 1.3		1.7 - 1.9		
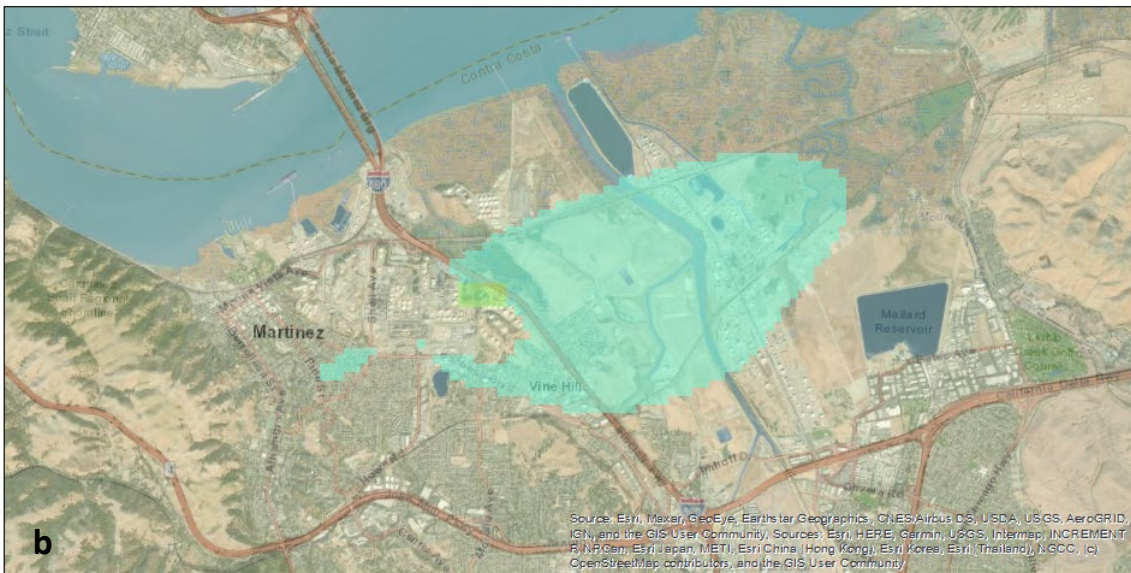
Figure ES.3: Three-year (2016–2018) average CALPUFF-simulated $PM_{2.5}$ concentrations for: (a) the 100-m receptor domain, and (b) a zoomed-in area of high concentrations. Emissions from the FCCU only (with an assumed WGS) are included in these simulations. Concentrations inside the PBF fence line and that are below 0.1 $\mu g/m^3$ are not shown.

List of Acronyms

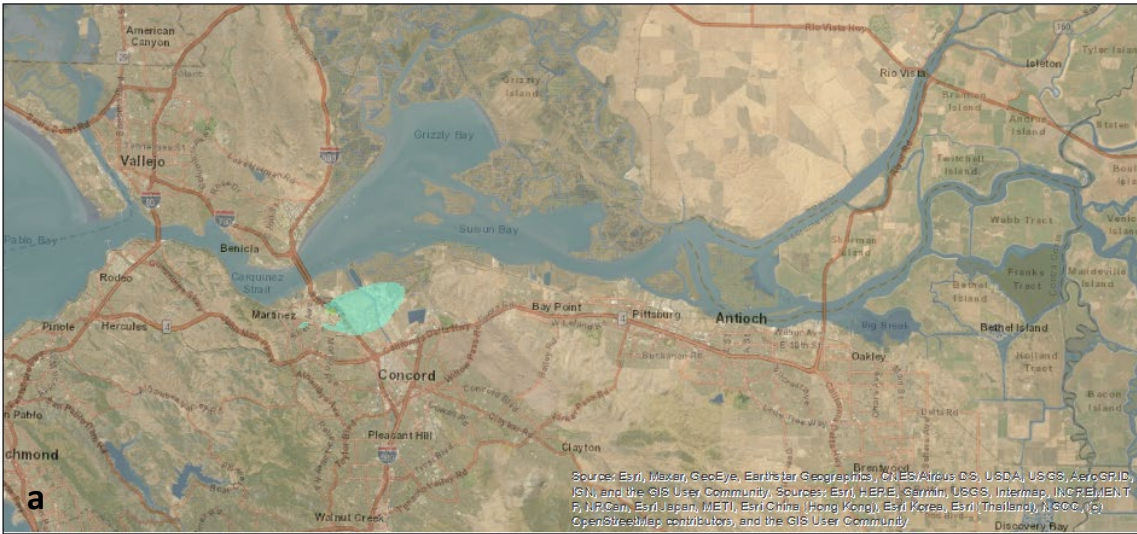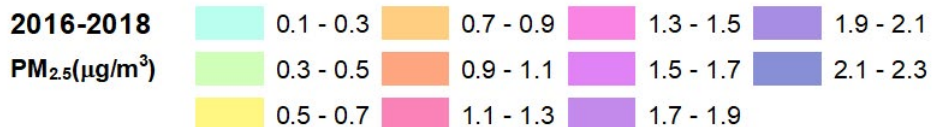|	
AB 617	Assembly Bill 617
AERMOD	American Meteorological Society/Environmental Protection Agency Regulatory Model
ASPEN	Assessment System for Population Exposure Nationwide (model)
BAAQMD	Bay Area Air Quality Management District
BenMAP-CE	Benefits Mapping and Analysis Program-Community Edition
CALPUFF	California Puff (model)
CAMx	Comprehensive Air Quality Model with Extensions
CARB	California Air Resources Board
CFR	Code of Federal Regulations
CMAQ	Community Multiscale Air Quality (model)
EPA	Environmental Protection Agency
FCCU	Fluid Catalytic Cracking Unit
FDDA	Four-Dimensional Data Assimilation
FLM	Federal Land Manager
GMT	Greenwich Mean Time
GR/DSCF	Grains per Dry Standard Cubic Feet
IOA	Index of Agreement
ISCST3	Industrial Source Complex Short Term 3 (model)
MMIF	Mesoscale Model Interface
PDF	Probability Distribution Function
PG	Pasquill–Gifford
PM$_{2.5}$	Particulate Matter 2.5 micrometers or less in diameter
PST	Pacific Standard Time
QA	Quality Assurance
QC	Quality Control
RMSE	Root Mean Square Error
SCICHEM	Second-order Closure Integrated Puff with Chemistry (model)
SRDT	Solar Radiation/Delta-T
TIBL	Thermal Internal Boundary Layer
UTM-TOX	Urban Airshed Model for Toxics
WGS	Wet Gas Scrubber
WOEIP	West Oakland Environmental Indicators Project
WRF	Weather Research and Forecasting (model)

Modeling Fine Particulate Matter Emissions
From the PBF Martinez Refinery:
An Air Quality Analysis
(Interim DRAFT Report – Version 2)

1   Introduction

1.1   Background

The adoption of Assembly Bill 617 (AB 617) established collaborative programs to reduce community exposure to air pollutants in neighborhoods most impacted by air pollution. Air District staff have been working closely with the California Air Resources Board (CARB), other state agencies, local air districts, community groups, community members, environmental organizations, regulated industries, and other key stakeholders to reduce harmful air pollutants in Bay Area communities.

As part of these programs, staff at the Bay Area Air Quality Management District (Air District or BAAQMD) plan to estimate contributions of directly emitted fine particulate matter ($PM_{2.5}$) from major industrial facilities in the Bay Area to ambient $PM_{2.5}$ levels. Staff will then analyze human exposure to resulting $PM_{2.5}$ levels. The California Puff (CALPUFF) model (Version 6.42; Exponent, 2011) will be used for estimating ambient $PM_{2.5}$ levels contributed by major facilities.

Emissions from each major facility will be separately simulated using CALPUFF. Two sets of receptor domains will be established. One will cover the entire Bay Area at 1-km grid resolution and the other will cover areas with concentrations above 0.1 µg/m^3 at 100-m grid resolution.

CALPUFF will be applied for three years (2016, 2017, and 2018) using year-specific meteorology and the same base-year (2018) emission estimates. Average results from the three annual simulations will be used for analyses to minimize the impact of year-to-year variability in meteorology on ambient $PM_{2.5}$ levels. The model estimates hourly concentrations at each receptor location, and these hourly values are then aggregated into daily, monthly, and annual averages. Concentrations estimated for these averaging periods will be analyzed for the purpose of model evaluation; however, only annual and three-year average concentrations will be presented in modeling reports for each facility.

CALPUFF is an advanced puff model originally developed for CARB (under the management of Saffet Tanrikulu, currently a District manager) to simulate pollutants emitted from major facilities and roadways in a complex terrain environment. CALPUFF was adopted by the U.S. Environmental Protection Agency (EPA) in 2003 as a "preferred" dispersion model, becoming one of the most widely used models for studying pollutant dispersion and transport in the U.S. and worldwide. However, in 2017, CALPUFF was removed from the U.S. EPA's "preferred model" list due to concerns about its ability to handle long-range pollutant transport. Because

the main goal of our project is to assess impacts of pollutants relatively near their sources, the U.S. EPA's concern is not relevant to our application of the model.

This report will present results from the application of CALPUFF to emissions from the PBF refinery in Martinez. Results for the Chevron refinery have previously been reported. CALPUFF applications for other Bay Area refineries and the Lehigh Cement factory are under way, and results from those simulations will be reported in subsequent documents.

1.2   Model Selection and Modeling Strategy

Air District staff have applied the U.S. EPA's Community Multiscale Air Quality (CMAQ) model (EPA, 1999) to estimate regional $PM_{2.5}$ and air toxics concentrations in the Bay Area (Tanrikulu et al., 2019). Because of limitations in its internal parameterization, this model is typically applied at 1-km or coarser grid resolutions. CMAQ has a plume-in-grid module for handling diffusion and dispersion of pollutants emitted from large point sources at subgrid scales. This plume-in-grid module employs a modified version of the Second-order Closure Integrated Puff with Chemistry (SCICHEM) model (Karamchandani et al., 2014).

One advantage of applying CMAQ with the plume-in-grid module is the ability to simultaneously simulate $PM_{2.5}$ at regular grid resolutions as well as subgrid resolutions. The plume-in-grid module in CMAQ was tested for the Bay Area modeling domain at 1-km grid resolution but failed to complete the test due to prohibitively large computational cost (Tanrikulu et al., 2019). Troubleshooting the model was not feasible within this project schedule; however, as a corroborative analysis, we applied the stand-alone version of SCICHEM (Version 3.2.2; EPRI, 2019) for simulating impacts of $PM_{2.5}$ emissions from the Chevron refinery, and its results were compared against results obtained from CALPUFF. This analysis was documented in our previous report on the modeling study for the Chevron refinery. Results from the two models largely agree with each other. It is also documented in (Koo et al., 2000).

Air District staff have applied another dispersion model (AERMOD) for simulating $PM_{2.5}$ emissions from local sources to assess their impacts on community-scale $PM_{2.5}$ levels. Most recently, AERMOD was applied for a wide variety of emission sources in West Oakland (BAAQMD and WOEIP, 2019). The model is also used by the District to evaluate permit applications. AERMOD utilizes meteorological information, such as wind speed and direction, at or close to source locations only. This is a significant shortcoming of the model when it is used to simulate elevated point source emissions that can travel to downwind locations where near-source meteorological information is no longer representative.

The CALPUFF model is specifically designed to utilize meteorological information over the entire area where a plume is expected to travel. Therefore, CALPUFF is more suitable for simulating $PM_{2.5}$ from the major point sources identified for this project.

CALPUFF has been applied in the Bay Area by the Air District as well as CARB to support several prior projects. In 2008, CARB, in collaboration with the Air District, conducted a health risk

assessment study to evaluate the potential public health impacts of diesel $PM_{2.5}$ emissions in West Oakland (CARB, 2008). To estimate ambient $PM_{2.5}$ levels, the project team considered several air dispersion models, such as ISCST3, AERMOD, ASPEN, CALPUFF, UTM-TOX, and CAMx. CALPUFF was selected because of its ability to handle complex terrain impacts and better treat various emission sources at fine scales. In 2017, CALPUFF was used for a collaborative demonstration project by the Air District and U.S. EPA that assessed the impact of $PM_{2.5}$ precursor emissions in the Bay Area (BAAQMD, 2017).

CALPUFF can be run with two different domains: (1) a computational domain, and (2) a receptor domain. In the computational domain, the model calculates plume dynamics using input parameters such as emissions, as well as gridded meteorological, land use and terrain elevation data. In the receptor domain, the model samples estimated concentrations at specified receptor points. Receptor points can be either gridded, where the model samples concentrations at the center of each grid cell or placed at discrete locations specified by the user. In general, gridded receptors are used for large, facility-impacted areas and discrete receptors are used for sensitive locations such as hospitals, schools, facility fence lines, etc.

As mentioned above, for the purpose of this study, we defined two sets of gridded receptors surrounding the facility and ran the model sequentially for both sets. The first set of receptors covered the entire Bay Area at 1-km grid resolution. A second set of 100-m resolution receptors covered areas with annual average $PM_{2.5}$ levels above 0.1 $\mu g/m^3$, as identified from the 1-km simulation.

1.3   Exposure Analysis

Simulated concentrations show contributions of emissions to ambient $PM_{2.5}$ levels but do not provide information on human exposure to this pollutant. Human exposure to $PM_{2.5}$ is one of the parameters used by air quality planners, the AB 617 technical assessment team, and rule developers in their analyses.

Exposure refers to any contact between an airborne contaminant and a surface of the human body, either outer (such as the skin) or inner (such as respiratory tract epithelium). Therefore, exposure requires the simultaneous occurrence of two events: a pollutant concentration at a particular place and time, and the presence of a person at that place and time (Ott, 1985).

To estimate population exposure, both concentrations and population data are needed. For this purpose, we will use average simulated $PM_{2.5}$ concentrations for 2016–2018 as the pollutant concentration estimate. Population data will be downloaded from the U.S. Census Bureau for 2010[1] and projected to 2018 using U.S. EPA's Benefits Mapping and Analysis Program-Community Edition (BenMAP-CE Version 1.5; EPA, 2018). Demographic data with socioeconomic information will be used to address disparity issues such as environmental inequality. Results from the exposure analysis will be provided in an accompanying report.

---

[1] https://www2.census.gov/census_2010/04-Summary_File_1/

1.4   Analysis of Representativeness

PM$_{2.5}$ levels in the Bay Area can vary significantly from year to year due to variable weather patterns and the associated variations in pollutant transport. To account for year-to-year variability in modeled concentrations, we simulated three consecutive years (2016–2018) for this project. This will increase the representativeness of simulated PM$_{2.5}$ levels.

Although we did not conduct a comprehensive meteorological representativeness study, simulating three recent years should increase the representation of meteorology across multiple years and is consistent with EPA's Guideline on Air Quality Models (40 CFR Part 51), where the use of multiple years of meteorological data (up to five) is recommended to ensure worst-case conditions are sufficiently characterized in regulatory modeling applications.

2   Modeling Methods

2.1   Emissions Inventory Preparation

CALPUFF requires an emissions input file that includes detailed information for each modeled source, including source ID number, location coordinates, base elevation, stack height, stack diameter, gas exit velocity, gas exit temperature, and emissions rate. This section describes the datasets and processes used to develop CALPUFF-ready emissions inputs for the PBF refinery.

To support the implementation of District Regulation 11, Rule 18 (11-18): Reduction of Risk from Air Toxic Emissions at Existing Facilities (BAAQMD, 2018), the District has begun collecting updated stack parameter information from permitted sources in the Bay Area. In addition, updated emission estimates for permitted facilities are being collected and reviewed under Regulation 12, Rule 15 (12-15, Petroleum Refining Emissions Tracking). Using information collected under these regulations, the Air District's Engineering Division developed and shared updated data for the PBF refinery to support CALPUFF modeling.

The Air District's Modeling and Analysis Section identified 63 unique point sources that emit PM$_{2.5}$ at PBF and worked with the Engineering Division to map all PM$_{2.5}$ emissions to the proper release points with their associated stack characteristics. Because multiple emission sources are often routed to a common stack, a total of 37 unique release points were modeled at PBF. It should be noted that all emissions and stack parameter data represent the best available information at the time the modeling was conducted.

Prior to modeling, quality control (QC) checks were performed on the stack-level data. For example, source locations were plotted and reviewed. Minimum and maximum values for each stack parameter were also identified to make sure that all values fell within reasonable bounds (see Appendix A). In a few cases, stack parameters were flagged, reviewed with staff from the Engineering Division, and updated based on their feedback. After QC checks were complete, emissions and stack parameters for each modeled source were converted to a CALPUFF-ready

format using a Python script developed by the Modeling and Analysis Section.

Note that CALPUFF utilizes grid averaged terrain data provided through its meteorological input from the Weather Research and Forecasting (WRF) model. The base elevation for each source provided usually does not match grid averaged terrain elevation, and if these base elevations are used, some short stacks could be represented as emitting at or below ground level. A similar problem arises if the actual elevations of receptors are used rather than grid averaged terrain elevations. For example, receptors with elevations below the grid averaged terrain elevations are erroneously treated as underground receptors. To maintain consistency among source, receptor, and terrain elevations in CALPUFF, the base elevations were replaced with the WRF grid averaged terrain elevations, and grid averaged terrain elevations were also used for receptors.

Table 2.1.1 provides a summary of $PM_{2.5}$ emissions and stack parameters for all $PM_{2.5}$ sources at the PBF refinery. Annual $PM_{2.5}$ emissions from the facility total 463 tons. The single largest source, the fluid catalytic cracking unit (FCCU), is responsible for 65% of the annual $PM_{2.5}$ emissions (300 tons). The table also includes both the original base elevation data and the values from the WRF model grid averaged terrain data that were ultimately used for modeling.

Figure 2.1.1 shows the location of all 37 release points modeled in CALPUFF. The location of the FCCU is also identified in this figure (FCCU emissions are routed to three nearby stacks).

This study also evaluated the potential impact of installing a wet gas scrubber (WGS) on the FCCU at PBF. This type of control equipment not only reduces PM emissions, but also alters the release characteristics of the emissions plume. To develop adjusted emissions and stack parameters for the FCCU with an assumed WGS for modeling purposes, staff from the District's Rule Development section reviewed source test data from other refineries. The goal of this review was to identify facilities with FCCU exhaust flow rates similar to the FCCU exhaust stacks at the PBF refinery, and that have WGS devices installed on the FCCU. Staff located four facilities with source test data to support this analysis:

- Hovensa Refinery, US Virgin Islands: test data from a US EPA 2011 Refinery Sector Information Collection Request
- Marathon Refining, Garyville, LA: 2017–2019 source test reports from the Louisiana Department of Environmental Quality's Electronic Document Management System
- Marathon Refining, Galveston Bay, TX: 2016 source test report from the Texas Commission on Environmental Quality's Central Registry
- Valero Refinery, Benicia, CA: 2016–2018 source test review memos from BAAQMD

Stack parameters for WGS-equipped FCCUs at these four facilities are shown in Table 2.1.2, along with average values across all these facilities. These average parameters were used to model FCCU emissions for the WGS control case, with all emissions routed to a single stack rather than the 3 stacks used to model FCCU emissions in the baseline scenario. This approach was used because it was assumed that the installation of a WGS would result in a single release

point for controlled FCCU emissions. The location of the central FCCU stack from the baseline scenario (Source S-1509 in Table 2.1.1) was used to represent this single stack for the WGS control case. In addition, a control factor of 78% was applied to PBF's baseline FCCU emissions, reducing annual $PM_{2.5}$ emissions from 300 tons to 66 tons. This control factor for $PM_{2.5}$, also provided by the District's Rule Development section, was based on an emission limit of 0.010 grains per dry standard cubic feet (gr/dscf).

Table 2.1.1: Stack parameters and PM$_{2.5}$ emissions for all PM$_{2.5}$ sources at PBF.

Source ID	Source Description	Base Elevation (m)	Gridded Terrain Elevation (m)	Stack Height (m)	PM2.5 Emissions (tons/year)	Contribution to PM$_{2.5}$ Emissions
S-1426	FCCU – Stack 1	16.45	18.39	49.38	99.87	21.6%
S-1426	FCCU – Stack 2	16.41	18.39	49.38	99.87	21.6%
S-1426	FCCU – Stack 3	16.41	18.39	49.38	99.87	21.6%
—	*FCCU Total*				*299.61*	*64.7%*
S-1507	CO Boiler #1*	16.45	18.39	49.38	4.38	0.9%
S-1509	CO Boiler #2*	16.41	18.39	49.38	3.97	0.9%
S-1512	CO Boiler #3*	16.41	18.39	49.38	4.33	0.9%
S-1486	F40 Heater (Chimney 1)	16.44	18.39	107.00	25.11	5.4%
S-1487	F41B Heater (Chimney 1)					
S-1488	F41A Heater (Chimney 1)					
S-1490	F43 Heater (Chimney 1)					
S-1491	F44 Heater (Chimney 1)					
S-1492	F45 Heater (Chimney 1)					
S-1493	F46 Heater (Chimney 1)					
S-1494	F-47/DH Heater (Chimney 1)					
S-1495	F49 Heater (Chimney 1)					
S-1496	F50 Heater (Chimney 1)					
S-1497	F51 Heater (Chimney 1)					
S-1498	F52 Heater (Chimney 1)					
S-1499	F53 Heater (Chimney 1)					
S-4161	H-101/HP3 Individual Heater	7.40	10.36	61.00	23.22	5.0%
S-4192	CTG2 Turbine	16.40	18.39	74.00	21.17	4.6%
S-4193	Heat Recovery Steam Generator #2					
S-4190	CTG1 Turbine	16.42	18.39	74.00	19.71	4.3%
S-4191	Heat Recovery Steam Generator #1					
S-1500	F55 Heater (Chimney 2)	16.47	18.39	107.00	11.30	2.4%
S-1502	F57 Heater (Chimney 2)					

S-1503	F58 Heater (Chimney 2)					
S-1504	F59 Heater (Chimney 2)					
S-1505	F60 Heater (Chimney 2)					
S-1515	DH F-71 HCU First-Stage Reboil (Chimney 2)					
S-1761	F-104/OPCEN Individual Heater	23.93	10.36	55.00	10.17	2.2%
S-1457	LOP Cooling Tower	14.63	18.39	20.58	9.15	2.0%
S-1778	OPCEN Cooling Tower	21.95	10.36	20.58	5.32	1.1%
S-1501	F56 Thermal Oxidizer	16.41	18.39	107.00	5.27	1.1%
S-1506	F-61/CP Individual Heater					
S-1508	F-63/CP Individual Heater					
S-1510	F-66/CP Individual Heater					
S-1511	F-67/CP Individual Heater					
S-1517	F77 Thermal Oxidizer					
S-4002	F-13425A/DCU Individual Heater	8.16	10.36	76.00	3.71	0.8%
S-4003	F-13425B/DCU Individual Heater					
S-1763	F-126/DH Individual Heater	16.50	18.39	67.00	3.55	0.8%
S-1771	Flexigas Flare	24.02	10.36	23.00	2.34	0.5%
S-1760	F102/OPCEN Individual Heater	24.09	18.39	46.00	2.29	0.5%
S-1762	F-128/DH Individual Heater	16.47	18.39	57.00	1.88	0.4%
A-100	MVR_ThermOx Individual Heater	0.45	10.25	14.94	1.07	0.2%
S-4210	DCD Cooling Tower	6.40	18.39	20.58	0.80	0.2%
S-4021	F-13909/DHT Individual Heater	8.24	18.39	46.02	0.72	0.2%
A-4181	F14610 Thermal Oxidizer	23.93	18.39	46.00	0.66	0.1%
S-4031	HGHT-Reboiler Heater (F-14012)	8.12	18.39	46.00	0.62	0.1%
S-4141	HGHT-Feed Heater (F-14011)					
S-601	Vapor Recover 2 Flare	9.54	15.31	21.34	0.58	0.1%
S-1470	LPG Flare	8.69	10.25	25.00	0.56	0.1%
S-6051	Diesel Engine, emergency standby	10.01	18.39	2.44	0.54	0.1%
S-6073	Portable Emergency Standby Diesel Fire Pump Engine	21.22	10.36	3.20	0.27	0.1%
A-2023	F109 Thermal Oxidizer	23.88	18.39	46.00	0.16	0.0%

S-6054	Diesel Engine, emergency standby	38.83	20.53	2.44	0.14	0.0%
S-4201	Clean Fuels Flare	12.94	10.36	10.00	0.14	0.0%
S-6052	Diesel Engine, emergency standby	34.21	20.53	2.44	0.13	0.0%
S-1471	LOP Flare	8.64	18.39	15.00	0.13	0.0%
S-6053	Diesel Engine, emergency standby	8.48	15.31	2.44	0.09	0.0%
S-603	Vapor Recover 1 Flare	17.78	18.39	19.81	0.05	0.0%
S-1772	OPCEN Flare	24.00	10.36	31.00	0.02	0.0%
S-602	Vapor Recover 3 Flare	12.59	18.39	13.72	0.02	0.0%
S-4005	DCU Coke Loading	8.30	10.36	18.59	0.01	0.0%
S-1481	F30/F31 OPCEN Individual Heater	26.63	18.39	12.00	0.00	0.0%
	Totals				**463.20**	**100.0%**

* Emissions from the CO boilers are routed to the same three stacks that the FCCU emissions are split across; therefore, total emissions from these three stacks are 312 tons/year (300 tons/year from the FCCU and 12 tons/year from the CO boilers).
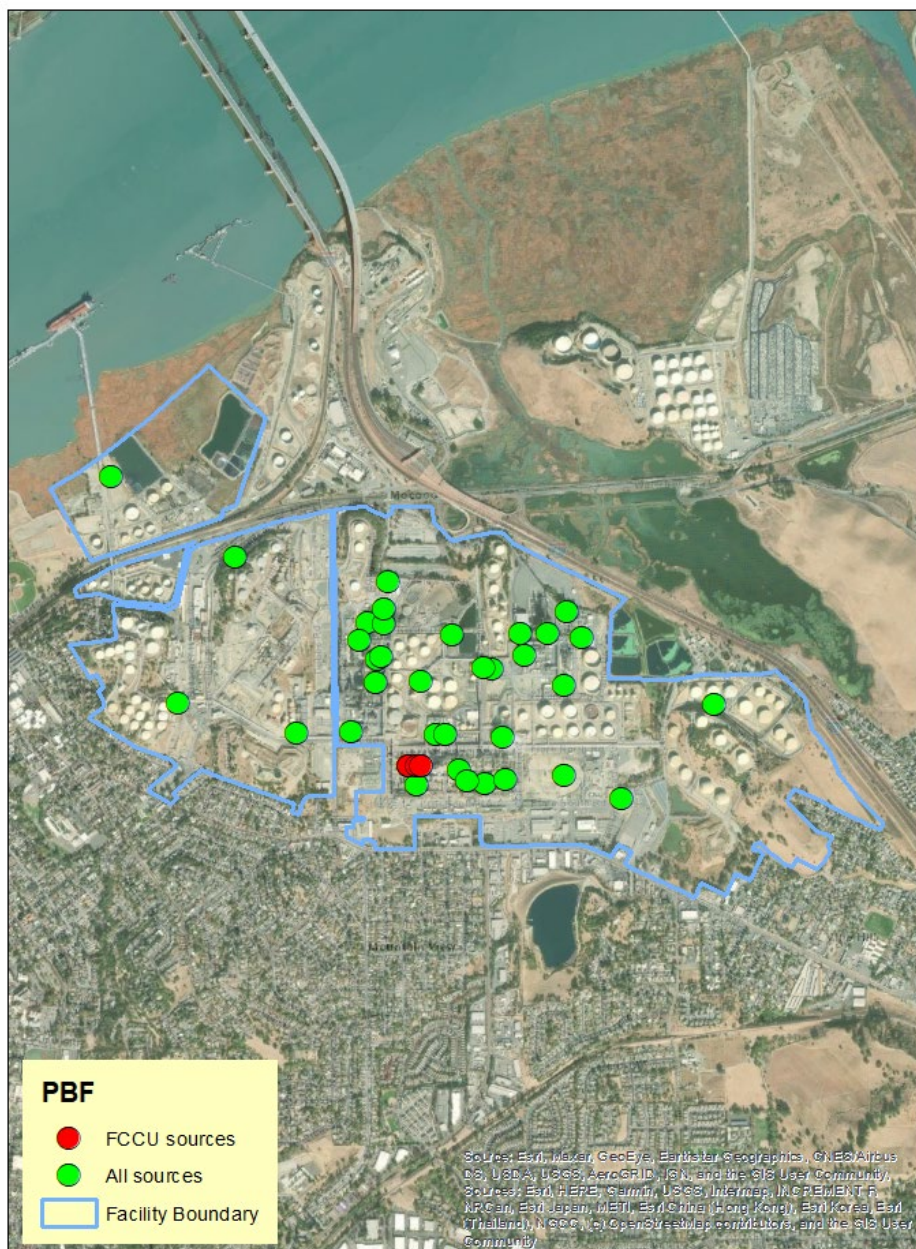
Figure 2.1.1: Locations of all 37 unique release points modeled at PBF. FCCU emissions are routed to three nearby stacks (shown in red).

Table 2.1.2: Stack parameters for a FCCU with a WGS installed.

Facility	Stack Diameter (m)	Stack Height (m)	Stack Temperature (°K)	Exit Velocity (m/sec)
Hovensa Refinery, US Virgin Islands (2011)	3.35	69.34	333.71	20.09
Marathon Refining, Garyville, LA (2017–2019)	3.96	68.88	337.76	11.87
Marathon Refining, Galveston Bay, TX (2016)	4.21	82.60	350.37	16.29
Valero Refinery, Benicia, CA (2016–2018)	—	73.00	326.48	—
Average	**3.84**	**73.46**	**337.08**	**16.08**

2.2   Meteorological Modeling

The WRF model (Version 4.1; Skamarock et al., 2019) was used to prepare meteorological inputs to CALPUFF. Four nested domains were used (Figure 2.2.1). The outer domain covered the entire western United States at 36-km horizontal grid resolution to capture synoptic (large-scale) flow features and the impact of these features on local meteorology. The second domain covered California and portions of Nevada at 12-km horizontal resolution to capture mesoscale (subregional) air flow features and their impacts on local meteorology. The third domain covered Central California at 4-km resolution to capture localized air flow features. The 4-km domain included the Bay Area, San Joaquin Valley, and Sacramento Valley, as well as portions of the Pacific Ocean and the Sierra Nevada range. The fourth domain covered the Bay Area and surrounding regions at 1-km resolution. All four domains employed 50 vertical layers, with the layer thickness increasing with height from the surface to the top of the modeling domain (about 18 km).
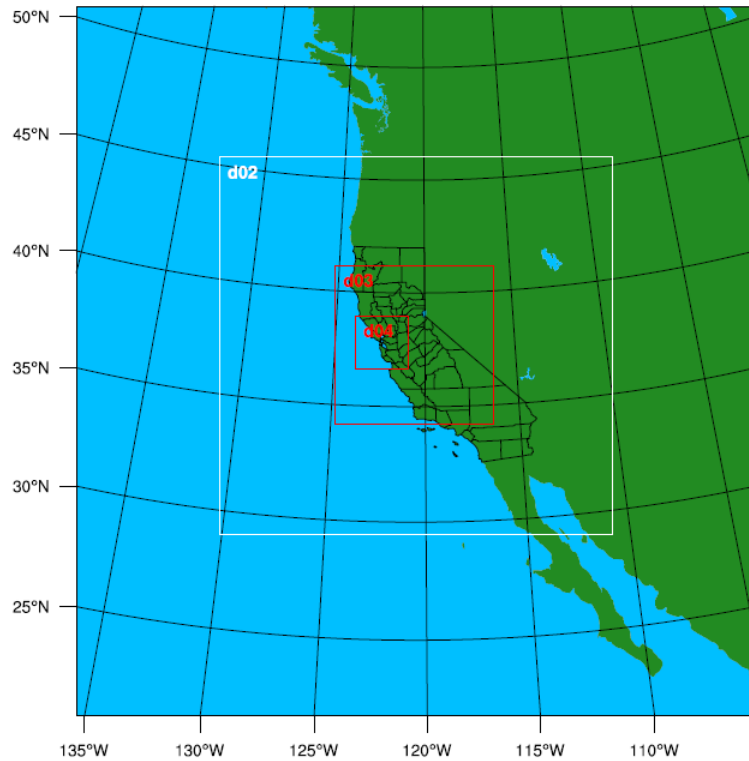
Figure 2.2.1: Nested WRF modeling domains.

The WRF model was tested using available options for physics and dynamics, as well as the datasets used to initialize and drive the model. Options tested included: (1) planetary boundary layer processes, (2) land surface processes, (3) four-dimensional data assimilation (FDDA) strategies, (4) horizontal and vertical diffusion algorithms, (5) advection schemes, and (6) initial and boundary conditions. Results of each test were evaluated, and the best-performing set of options was selected for final modeling.

WRF was applied for 2016, 2017, and 2018. Observed winds and temperatures were ingested into the model as the simulations were performed to increase the representation of local and regional meteorology. Table 2.2.1 provides a summary of annual mean model performance at five observation stations, from Vallejo in the north to San Jose in the south. The performance displayed is typical for the WRF model when it is applied over complex terrain. Variability in station performance is relatively small from year to year and fairly consistent among stations as well.

Example results from the rigorous model evaluation of WRF are provided in Appendix B. The first example shows simulated and observed time series plots of winds and temperatures at the PBF East meteorological monitoring tower and a comparison between them. The second example shows vertical profiles of simulated and observed temperature and humidity at the Oakland upper air meteorological station for summer and winter days of 2018. A brief discussion on the comparison between simulated and observed fields is also provided in Appendix B.

Table 2.2.1: A summary of the statistical evaluation of WRF for 2016–2018.

2016			PBF East	San Jose	Oakland	San Pablo	Vallejo
Wind Speed	Bias	(m/s)	0.00	−1.45	−1.63	−0.44	−0.26
Wind Speed	Gross Error	(m/s)	0.92	1.55	1.80	1.71	0.80
Wind Speed	RMSE	(m/s)	1.14	1.84	2.13	2.02	0.96
Wind Speed	IOA		0.67	0.61	0.59	0.59	0.68
Wind Direction	Bias	(deg)	8.18	16.78	2.37	−2.25	0.50
Wind Direction	Gross Error	(deg)	44.14	41.68	31.99	34.04	33.58
Temperature	Bias	(°K)	0.50	0.77	0.23	0.71	0.84
Temperature	Gross Error	(°K)	1.25	1.35	1.20	1.49	1.42
Temperature	RMSE	(°K)	1.51	1.61	1.46	1.79	1.70
Temperature	IOA		0.92	0.92	0.90	0.84	0.90
2017			PBF East	San Jose	Oakland	San Pablo	Vallejo
Wind Speed	Bias	(m/s)	0.15	−1.32	−1.47	−0.71	−0.09
Wind Speed	Gross Error	(m/s)	0.91	1.44	1.68	1.62	0.77
Wind Speed	RMSE	(m/s)	1.13	1.73	2.03	1.97	0.94
Wind Speed	IOA		0.67	0.64	0.60	0.58	0.68
Wind Direction	Bias	(deg)	6.77	20.42	−1.35	−1.41	−0.16
Wind Direction	Gross Error	(deg)	45.92	42.99	33.55	35.95	36.22
Temperature	Bias	(°K)	0.38	0.57	0.47	0.59	0.73
Temperature	Gross Error	(°K)	1.33	1.32	1.40	1.52	1.48
Temperature	RMSE	(°K)	1.59	1.58	1.67	1.81	1.76
Temperature	IOA		0.92	0.92	0.88	0.85	0.90
2018			PBF East	San Jose	Oakland	San Pablo	Vallejo
Wind Speed	Bias	(m/s)	0.03	−1.34	−1.50	−0.77	−0.24
Wind Speed	Gross Error	(m/s)	0.87	1.44	1.67	1.56	0.76
Wind Speed	RMSE	(m/s)	1.06	1.72	2.00	1.87	0.93
Wind Speed	IOA		0.66	0.63	0.59	0.58	0.69
Wind Direction	Bias	(deg)	10.67	11.95	0.35	−1.28	−2.80
Wind Direction	Gross Error	(deg)	47.11	39.04	33.34	36.22	34.03
Temperature	Bias	(°K)	0.54	0.60	1.09	0.72	0.70
Temperature	Gross Error	(°K)	1.44	1.29	1.45	1.64	1.47
Temperature	RMSE	(°K)	1.73	1.56	1.78	1.96	1.78
Temperature	IOA		0.92	0.93	0.88	0.84	0.91

2.3   Application of CALPUFF

Meteorological inputs to CALPUFF were prepared using outputs from the WRF model. The Mesoscale Model Interface (MMIF) computer program (Version 3.4.1; Brashers and Emery,

2019) was used for this purpose. This program extracts parameters from WRF outputs that are needed as CALPUFF inputs, such as wind speed, temperature, mixing height, surface roughness length, land use category, terrain elevation, and leaf area index.

MMIF provides two options for diagnosing the gridded Pasquill–Gifford (PG) stability classes required by CALPUFF. The first option is called the Solar Radiation/Delta-T (SRDT) method, which derives the PG stability class based on wind speed, solar radiation, and temperature (EPA, 1993). The second option derives the stability class from the parameterization of relationships between Monin–Obukhov lengths and surface roughness (Golder, 1972). The second option was selected for this project, and this choice is consistent with recent BAAQMD AERMOD applications in West Oakland.

CALPUFF uses far fewer vertical layers than WRF. MMIF performs a down-scaling of high resolution WRF layers to CALPUFF layers. CALPUFF layers used in this study were based on recommendations developed by modelers from the EPA and the Federal Land Manager (FLM) community (EPA, 2009). The layer definition is shown in Table 2.3.1.

Table 2.3.1: CALPUFF layers above ground level.

Layer	Layer Top Height (m)
1	20
2	40
3	80
4	160
5	320
6	640
7	1,200
8	2,000
9	3,000
10	4,000

CALPUFF provides many options for selecting model processes, such as wet scavenging, dry deposition, stack tip downwash, and building downwash. These options can be selected and assigned a value; if not selected, no value is assigned. The available options were carefully reviewed and selected for handling complex terrain with diverse meteorological conditions. The selected options and their values are shown in Appendix C.

CALPUFF simulations were performed for three years (2016–2018) and for two receptor grid configurations. The first simulation used 1-km computational and receptor domains over the entire Bay Area and included emissions from all point sources at the PBF facility. Annual average $PM_{2.5}$ concentrations were estimated for each year. The purpose of this simulation was to identify the areal extent of annual average concentrations exceeding 0.1 $\mu g/m^3$.

The second simulation used 1-km computational and 100-m receptor domains over the area for

which annual average concentrations exceeded 0.1 $\mu g/m^3$ from the first simulation. A 5-km buffer zone was established between areas with concentrations exceeding 0.1 $\mu g/m^3$ and boundaries of the 100-m receptor domain to minimize boundary impacts on estimated concentrations. The second simulation also included emissions from all point sources at this facility. The purpose of the second simulation was to increase the density of receptors at locations where $PM_{2.5}$ concentrations were highest.

Additional simulations were conducted that used the same computational and receptor domains as the second simulation, but only included $PM_{2.5}$ emissions from the FCCU (with and without a WGS installed) at PBF.

Figure 2.3.1 shows the 1-km (gray box) and 100-m (red box) receptor domains used for all simulations. This figure also shows three-year (2016–2018) average $PM_{2.5}$ concentrations at 1-km receptor resolution that included emissions from all point sources at the PBF facility.

For all simulations, background (regional) concentrations and incoming pollutants through boundaries of the modeling domain were set to zero. In other words, estimated concentrations are entirely from facility emissions.
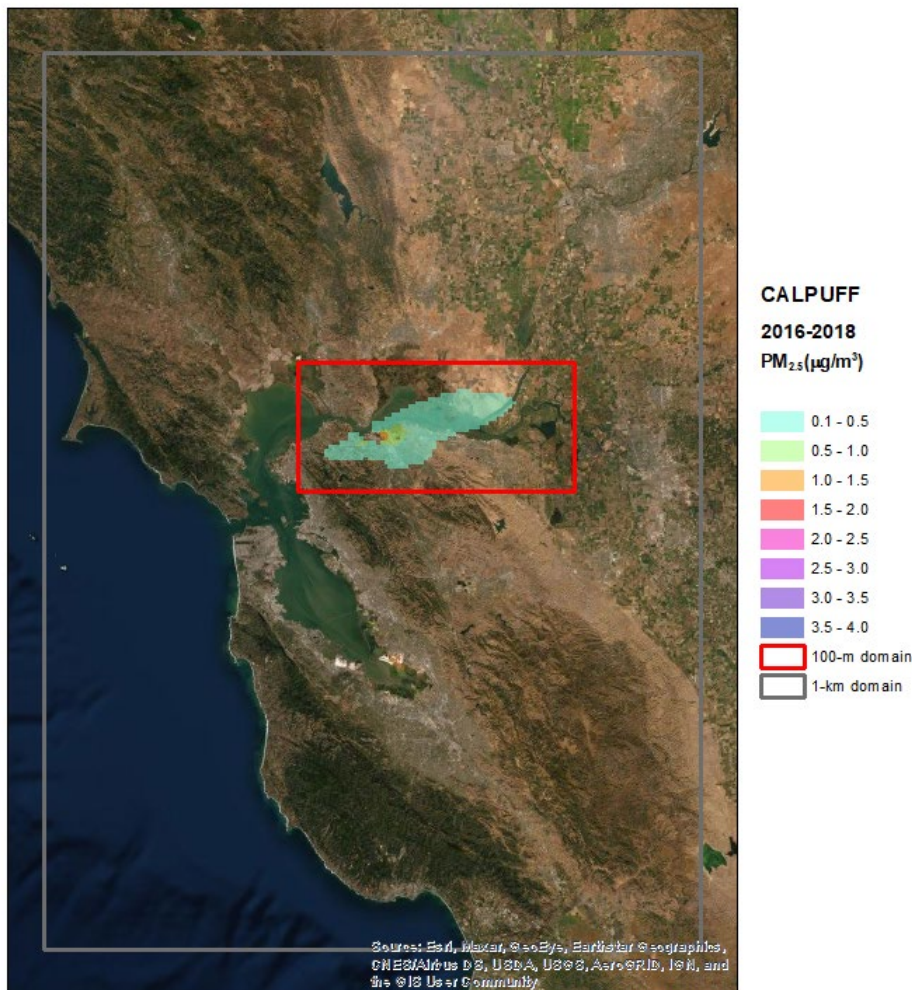
Figure 2.3.1: The gray and red boxes show the 1-km and 100-m receptor domains, respectively. CALPUFF-simulated three-year average PM$_{2.5}$ concentrations are also shown.

3 Results

3.1 Simulations with Emissions from All Sources

Figure 3.1.1 shows the three-year (2016–2018) average CALPUFF-simulated PM$_{2.5}$ concentrations for the 100-m receptor domain. Estimated concentrations within the PBF facility fence line are not shown. Estimated concentrations below 0.1 µg/m^3 are also excluded.

CALPUFF estimates concentrations at receptor points located at the center of each 100 x 100 m grid cell. For mapping purposes, each grid cell is color coded based on the concentration value at its center. An interval of 0.5 µg/m^3 was selected for color coding (except for concentrations between 0.1 µg/m^3 and 0.5 µg/m^3).

As can be seen in Figure 3.1.1a, the lowest concentration bin (0.1 μg/m^3 to 0.5 μg/m^3) extends from Pleasant Hill in the south to Birds Landing in the north and from Pinole Valley in the west to Decker Island in the east. The emissions plume has an elongated shape in the southwesterly and northeasterly directions from Martinez, consistent with the predominant winter and summer wind patterns there, respectively.

The area with concentrations above 0.5 μg/m^3 is much smaller than the area covered by the lowest concentration bin, as described above. These higher concentrations are mostly confined to the area around the PBF facility and extend toward the northeast of the facility.

To better visualize the high-concentration areas, a zoomed-in map of the 100-m receptor domain was created (see Figure 3.1.1b). As shown in this figure, an area with concentrations between 0.5 μg/m^3 and 1.0 μg/m^3 extends from the east side of the facility toward Port Chicago, between the southern bank of Suisun Bay and California Highway 4. There is also a small area with concentrations between 0.5 μg/m^3 and 1.0 μg/m^3 to the west of the facility.

Concentrations above 1.0 μg/m^3 primarily lie to the east of the facility, with no overlap of residential areas in the region. In addition, a sharp concentration gradient is apparent near the facility fence line. The maximum concentration (3.8 μg/m^3) is located just outside the fence line.

Additional analyses on the modeling results are presented in Appendix D.

PBF

2016-2018 PM$_{2.5}$(μg/m^3)

0.1 - 0.5	1.0 - 1.5	2.0 - 2.5	3.0 - 3.5
0.5 - 1.0	1.5 - 2.0	2.5 - 3.0	3.5 - 4.0

PBF

2016-2018 PM$_{2.5}$(μg/m^3)

0.1 - 0.5	1.0 - 1.5	2.0 - 2.5	3.0 - 3.5
0.5 - 1.0	1.5 - 2.0	2.5 - 3.0	3.5 - 4.0
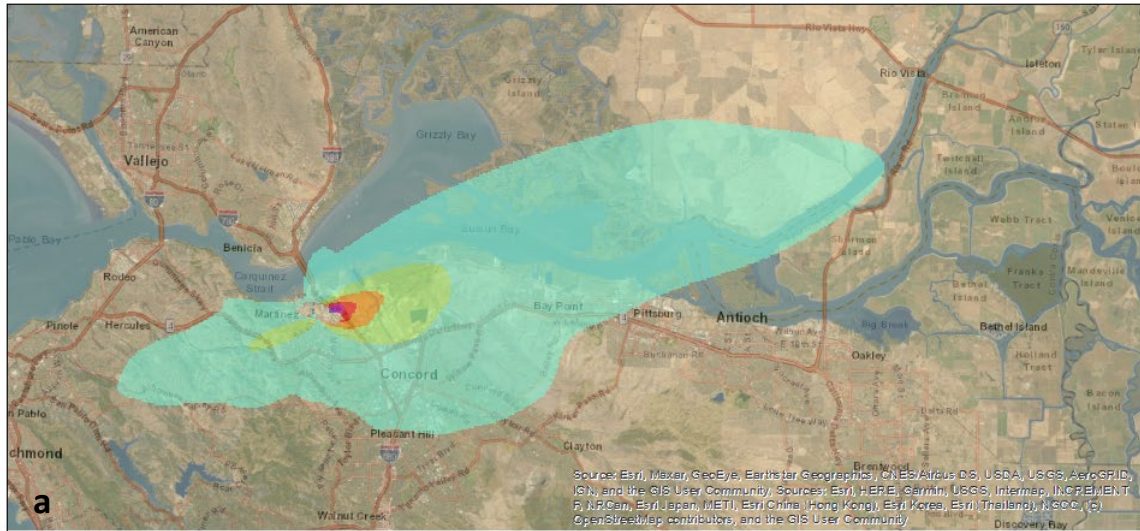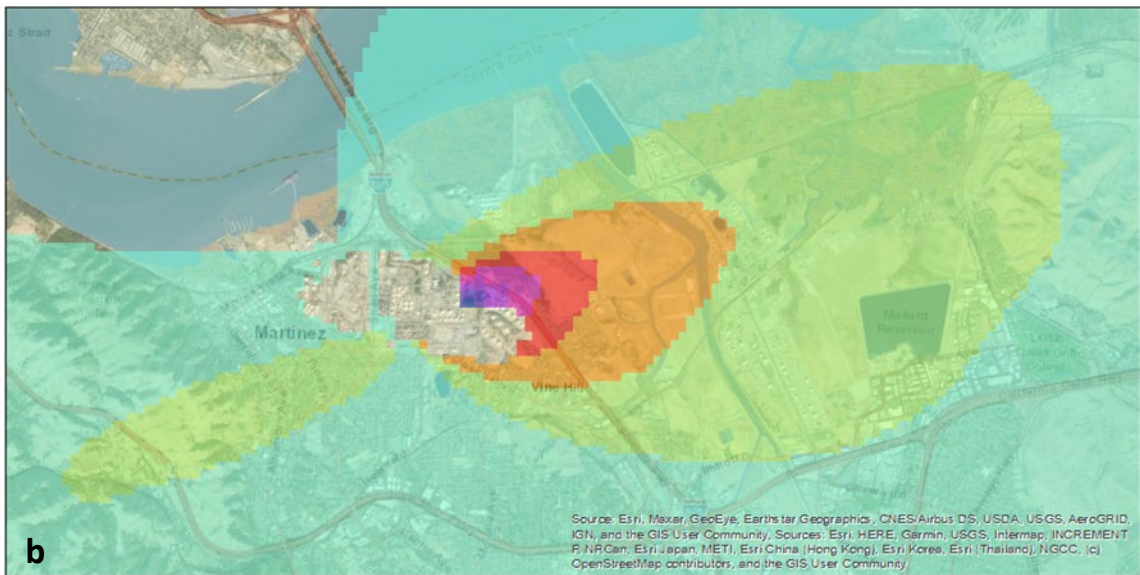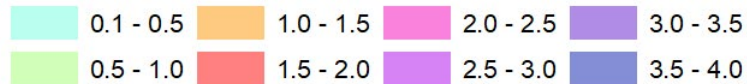
Figure 3.1.1: Three-year (2016–2018) average CALPUFF-simulated PM$_{2.5}$ concentrations for (a) the 100-m receptor domain, and (b) a zoomed-in area of highest concentrations. Emissions from all PBF point sources are included in this simulation. Concentrations inside the PBF fence line and that are below 0.1 μg/m^3 are not shown.

3.2 Simulations with FCCU Emissions

CALPUFF was also run with emissions from the FCCU only under two scenarios: (1) baseline FCCU emissions with existing stack parameters and (2) with emissions consistent and stack parameters consistent with a WGS installed.[2] (See Section 2.1 for a discussion of WGS emissions.)The resulting three-year average $PM_{2.5}$ concentrations are shown in Figure 3.2.1 (baseline FCCU) and Figure 3.2.2 (FCCU with a WGS installed). Again, concentrations within the facility fence line and below 0.1 $\mu g/m^3$ are not shown. An interval of 0.2 $\mu g/m^3$ was selected for color coding concentration values at grid cells.

Emissions from this source are mainly transported to the southwest and northeast of the facility, similar to the all-source results, but with smaller impact areas. The number of receptors with three-year average concentrations above 0.1 $\mu g/m^3$ was reduced from 42,741 (all-source simulation) to 21,452 (FCCU-only simulation), i.e., a 50% reduction when a WGS is not installed. The maximum three-year average concentration from this source is 2.0 $\mu g/m^3$, or about 53% of the maximum concentration from the all-source simulation. This is slightly less than the contribution of the FCCU to total $PM_{2.5}$ emissions from the facility (65%).

Installation of a WGS further reduces the number of receptors with three-year average concentrations above 0.1 $\mu g/m^3$ to 1,078 (a 95% reduction from the baseline FCCU emission scenario) and the maximum three-year average concentration to 0.46 $\mu g/m^3$ (22% of the maximum concentration from the baseline FCCU emission scenario). This reduction in the maximum concentration is consistent with the emission reduction by a WGS (78%) as the maximum concentration occurs close to the source location.

Table 3.2.1 shows the key findings of simulations with the three sets of emissions.

Table 3.2.1: Key findings of simulations with emissions from all point sources, FCCU only, and FCCU with assumed WGS.

	Annual $PM_{2.5}$ emissions (tons/year)	Maximum simulated concentrations ($\mu g/m^3$)	Number of sampling receptors with concentrations above 0.1 $\mu g/m^3$
All point sources	463.20	3.8	42,741
FCCU only, baseline	299.61	2.0	21,452
FCCU with assumed WGS	65.91	0.46	1,078

---

[2] Note that a scenario for a less stringent emissions limit (0.02 grains per dry standard cubic foot) was developed by scaling concentrations from the baseline FCCU scenario.
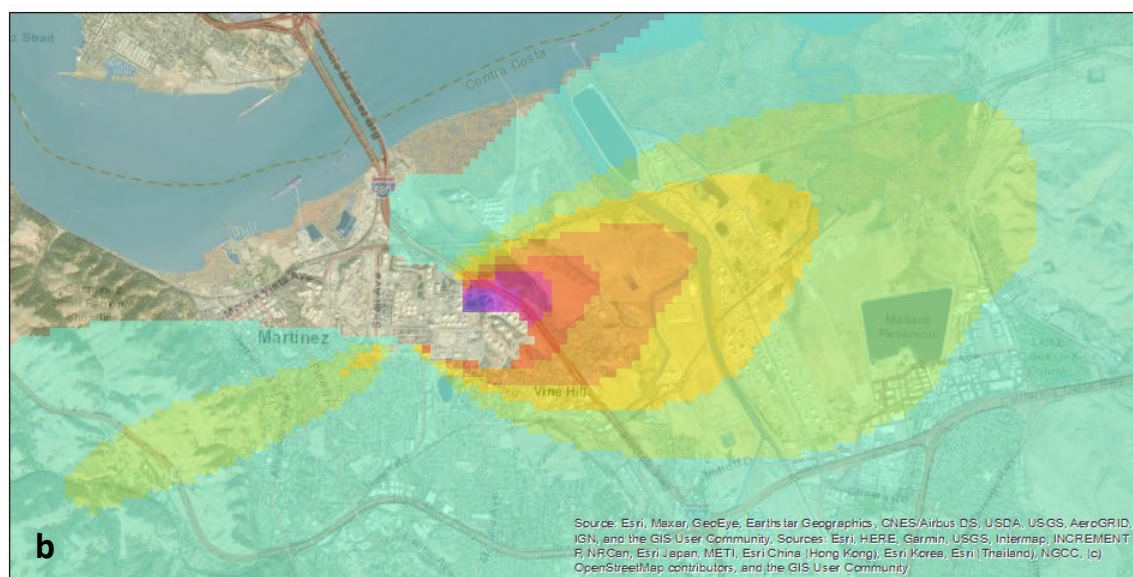
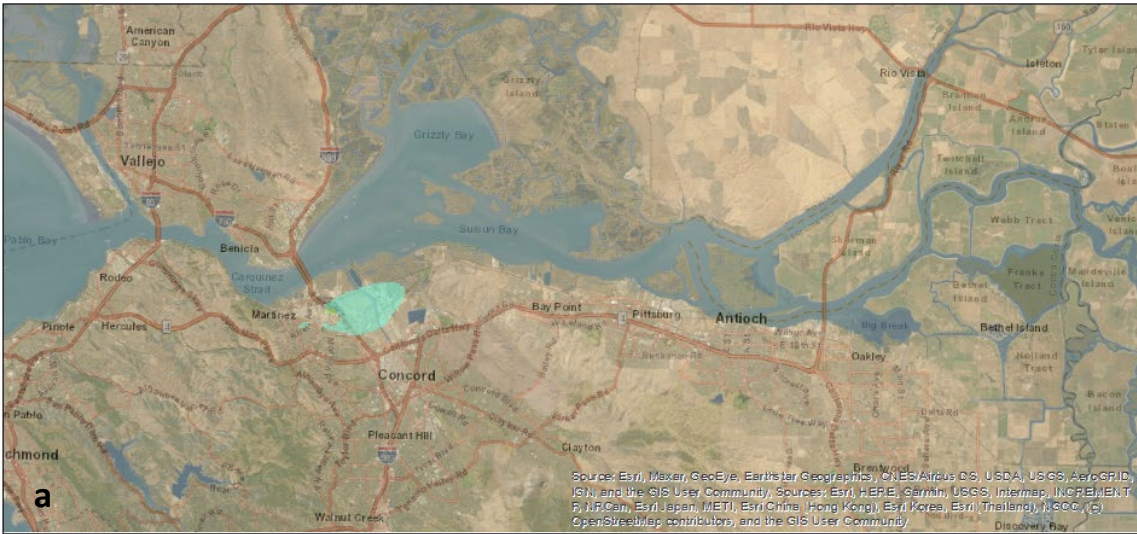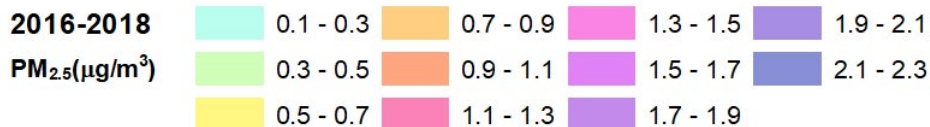Figure 3.2.1: Three-year (2016–2018) average CALPUFF-simulated PM$_{2.5}$ concentrations for: (a) the 100-m receptor domain, and (b) a zoomed-in area of high concentrations. Emissions from the FCCU only (without a WGS) are included in these simulations. Concentrations inside the PBF fence line and that are below 0.1 µg/m^3 are not shown.

PBF FCCU WGS

2016-2018		0.1 - 0.3		0.7 - 0.9		1.3 - 1.5		1.9 - 2.1
$PM_{2.5}(\mu g/m^3)$		0.3 - 0.5		0.9 - 1.1		1.5 - 1.7		2.1 - 2.3
		0.5 - 0.7		1.1 - 1.3		1.7 - 1.9		

PBF FCCU WGS

2016-2018		0.1 - 0.3		0.7 - 0.9		1.3 - 1.5		1.9 - 2.1
$PM_{2.5}(\mu g/m^3)$		0.3 - 0.5		0.9 - 1.1		1.5 - 1.7		2.1 - 2.3
		0.5 - 0.7		1.1 - 1.3		1.7 - 1.9		
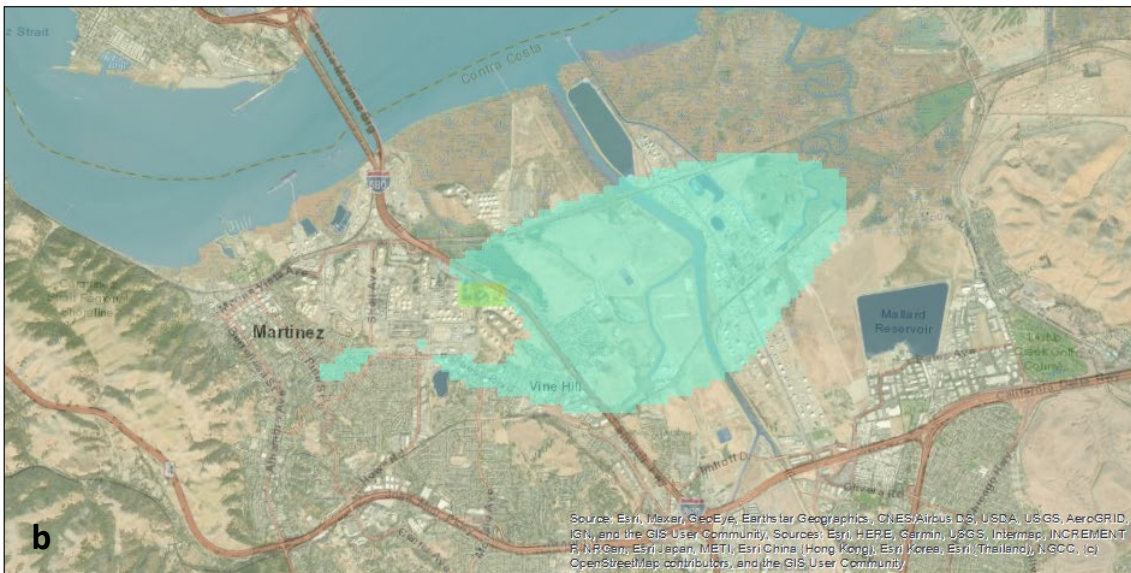
Figure 3.2.2: Three-year (2016–2018) average CALPUFF-simulated $PM_{2.5}$ concentrations for: (a) the 100-m receptor domain, and (b) a zoomed-in area of high concentrations. Emissions from the FCCU only (with an assumed WGS) are included in these simulations. Concentrations inside the PBF fence line and that are below 0.1 $\mu g/m^3$ are not shown.

4   Summary

The purpose of this project is to estimate contributions of directly emitted fine particulate matter from major industrial facilities in the Bay Area to ambient $PM_{2.5}$ concentrations. Project findings are expected to support the District's AB 617 program, providing technical information to decision makers, planners, the AB 617 technical assessment team, and rule developers.

We have previously estimated contributions of $PM_{2.5}$ emissions from the Chevron refinery, and in this study, we estimated contributions of emissions from the PBF refinery to ambient $PM_{2.5}$ levels for 2016–2018. Modeling analyses of the impacts of emissions from other Bay Area refineries and the Lehigh Cement factory will follow using an approach similar to the one used for the Chevron and PBF refineries.

The technical approach developed for this project was carefully evaluated. Options were weighed and discussed among the modeling team, and the strategy that was anticipated to provide the best modeling results was adopted. In addition, consideration was given to providing results that would address the needs of anticipated end users.

The opening sections of this document provide detailed information on the purpose of the project, model selection, and types of analyses conducted. This document also provides a summary of emissions and meteorological input preparation, model execution, analysis and interpretation of model outputs, and QA/QC performed.

Key findings of the project include:
- Simulating three years provides better representation of average concentrations.
- CALPUFF results show some differences among the years simulated, but overall characteristics of simulated $PM_{2.5}$ concentrations are consistent among the years.
- The single FCCU that accounts for about 65% of total $PM_{2.5}$ emissions from PBF contributes about 53% of the peak three-year average contributions from all PBF sources.
- Installation of a WGS, which reduces the FCCU emissions by 78%, reduces the peak three-year average contribution from the FCCU by the same percentage.
- The peak annual average $PM_{2.5}$ concentration is just outside the facility's northeastern fence line, but concentrations quickly diminish at a short distance away from the facility.
- Peak monthly average $PM_{2.5}$ concentrations are higher in summer than in winter due to stronger vertical mixing during the summer months.

5   References

BAAQMD, 2017. Demonstration of SO_2 Precursor Contributions to $PM_{2.5}$ in the San Francisco Bay Area. Bay Area Air Quality Management District. https://www.baaqmd.gov/~/media/files/planning-and-research/rules-and-regs/workshops/2017/reg-02/public-hearing/so2precursor_demonstration_final_report-pdf

BAAQMD, 2018. Regulation 11, Rule 18 – Reduction of risk from air toxic emissions at existing facilities. https://www.baaqmd.gov/~/media/dotgov/files/rules/regulation-11-rule-18-reduction-of-risk-from-air-toxic-emissions-at-existing-facilities/documents/20171115_fr_1118-pdf.pdf

BAAQMD and WOEIP, 2019. Owning Our Air – The West Oakland Community Action Plan. https://www.baaqmd.gov/community-health/community-health-protection-program/west-oakland-community-action-plan

Brashers, B., Emery, C., 2019. User's Manual: The Mesoscale Model Interface Program Version 3.4.1. Ramboll US Corporation. https://www3.epa.gov/ttn/scram/models/relat/mmif/MMIFv3.4.1_Users_Manual.pdf

CARB, 2008. Diesel Particulate Matter Health Risk Assessment for the West Oakland Community. California Air Resources Board. https://ww3.arb.ca.gov/ch/communities/ra/westoakland/documents/westoaklandreport.pdf

EPA, 1993. An evaluation of a solar radiation/delta-T method for estimating Pasquill–Gifford (P–G) stability categories. Technical Report prepared by the U.S. Environmental Protection Agency, Office of Air Quality Planning and Standards, Research Triangle Park, NC (EPA–454/R–93–055).

EPA, 1999. Science Algorithms of the EPA Models-3 Community Multiscale Air Quality (CMAQ) modeling system. EPA/600/R-99/030, March 1999. https://www.cmascenter.org/cmaq/science_documentation

EPA, 2009. Clarification on EPA-FLM recommended settings for CALMET. Memorandum prepared by the U.S. Environmental Protection Agency, Office of Air Quality Planning and Standards, Research Triangle Park, NC.

EPA, 2018. BenMAP: Environmental Benefits Mapping and Analysis Program-Community Edition User's Manual. July 2018. https://www.epa.gov/sites/production/files/2015-04/documents/benmap-ce_user_manual_march_2015.pdf

EPRI, 2019. SCICHEM Version 3.2.2: User's Guide. Electric Power Research Institute, Palo Alto, CA, December 2019.

Exponent, 2011. CALPUFF Modeling System Version 6 User Instructions.

Golder, D., 1972. Relations among stability parameters in the surface layer. *Boundary-Layer Meteorol.* **3**, 47–58. https://doi.org/10.1007/BF00769106

Karamchandani, P., Johnson, J., Yarwood, G., Knipping, E., 2014. Implementation and application of sub-grid-scale plume treatment in the latest version of EPA's third-generation air

quality model, CMAQ 5.01. *J. Air Waste Manage. Assoc.*, **64**, 453–467.
https://doi.org/10.1080/10962247.2013.855152

Koo, B., Jia, Y., Reid, S., Fang, Y., Matsuoka, J., 2020. High Resolution Modeling of Air Quality Impacts of Major Point Sources in the San Francisco Bay Area [Conference presentation]. A&WMA's 113th Annual Conference & Exhibition, San Francisco, CA, United States.

Ott, W. R., 1985. Total human exposure. *Environ Sci. Technol.* **19**, 880–886.
https://doi.org/10.1021/es00140a001

Skamarock, W. C., Klemp, J. B., Dudhia, J., Gill, D. O., Liu, Z., Berner, J., Wang, W., Powers, J. G., Duda, M. G., Barker, D. M., Huang, X.-Y., 2019. A Description of the Advanced Research WRF Version 4. NCAR Tech. Note NCAR/TN-556+STR. https://doi.org/10.5065/1dfh-6p97

Tanrikulu, S., Koo, B., Reid, S., Fang, Y., Jia, Y., Cordova, J., Matsuoka, J., 2019. Updating CMAQ's Plume-in-Grid Treatment for the SAPRC07TC Chemistry Mechanism. Bay Area Air Quality Management District, San Francisco, CA, January 2019.

Tanrikulu, S., Reid, S., Koo, B., Jia, Y., Cordova, J., Matsuoka, J., and Fang, y., 2019: Fine particulate matter Data Analysis and Regional Modeling in the San Francisco Bay Area to Support Ab617. BAAQMD Air Quality Modeling and Data Analysis Section Publication No: 201901-017-PM.

Tanrikulu, S., Koo, B., Reid, S., Fang, Y., Jia, Y., Cordova, J., Matsuoka, J., 2019: Air Toxics Data Analysis and Regional Modeling in the San Francisco Bay Area to Support Ab617. BAAQMD Air Quality Modeling and Data Analysis Section Publication No: 201903-019-Toxics.

Appendix A – Emissions Inventory Preparation

As described in the body of this report, QC checks were performed on stack parameters for PBF PM$_{2.5}$ sources prior to modeling. For example, a range check was performed on each stack parameter to ensure that all values fell within reasonable bounds. In a few cases, stack parameters were flagged and updated in consultation with staff from the Engineering Division. Table A.1 shows the results of range checks for the final set of stack parameters used in the CALPUFF modeling.

In addition, the base elevation and stack height for each modeled source were added to calculate an actual release point. These values were then compared with the vertical layer structure of the CALPUFF model to determine how emissions would be apportioned vertically. This comparison does not include plume rise.

About 352 tons of PM$_{2.5}$ (76% of the total) were being injected into CALPUFF layer 3, which begins at a height of 60 m and is 40 m thick (see Table A.2).

Table A.1: Results of range check for stack parameters assigned to PBF sources.

Parameter	Base Elevation (m)	Stack Height (m)	Stack Diameter (m)	Exit Temperature (°K)	Exit Velocity (m/s)	PM$_{2.5}$ Emissions (tons/year)
Minimum	10.25	2.44	0.15	293	1.80	0.0036
Maximum	20.53	107.00	5.76	1273	68.75	104.25

Table A.2: Results of mapping sources and emissions to CALPUFF layers.

CALPUFF Layer	Layer Height (m)	Layer Thickness (m)	Number of Sources	PM$_{2.5}$ Emissions (tons/year)
1	20	20	2	0.36
2	40	20	16	20.99
3	80	40	12	352.03
4	160	80	7	89.81
5	320	160		
6	640	320		
7	1,200	560		
8	2,000	800		
9	3,000	1,000		
10	4,000	1,000		

Appendix B – Meteorological Model Evaluation

The WRF model was applied for three years (2016–2018) and evaluated against available surface and upper air observations, especially for its 1-km modeling domain. Ramboll's METSTAT program[3] was used for evaluating the model against surface observations. This program compares hourly average WRF-simulated meteorological fields against observations, calculates statistical measures such as mean observation, mean simulation, bias, error, gross error, root-mean-square error (RMSE), and index of agreement, and then tabulates and graphically displays findings.

For evaluating the model against upper air measurements, a skew-T plot program was used. This program plots simulated and observed temperatures and humidity in the vertical direction.

A summary table of estimated statistical measures is provided in the main body of this document. Time series comparisons between simulated and observed wind speeds, wind directions, and temperatures are presented in Section B.1. Sample skew-T plots are presented in section B.2.

B.1 Time Series Comparisons

We compared simulated winds and temperatures against observations to evaluate the model. Even though the model was evaluated against available observations archived at the National Center for Atmospheric Research and in the District's Data Management System, only time series plots at the PBF facility are shown in this Appendix. To better show comparison details, time series plots are displayed for discrete calendar quarters.

Figures B.1 through B.9 show time series plots of daily average observed and WRF-simulated wind speeds, wind directions, and temperatures for 2016, 2017, and 2018, respectively. As these figures show, the WRF-simulated winds and temperatures match the observed trends exceptionally well for the whole simulation period. This good performance is due to the Modeling and Analysis Section's continuous evaluation of the WRF and efforts to improve model performance. Ingesting data from the relatively dense Bay Area observation network into the WRF also helps improve its performance. The WRF performance at PBF East is much better than that at Chevron—especially the temperature performance, which is consistently good for all three years. The systematic underestimation of wind speed at Chevron during the summer months is not noticeable at PBF. The PBF facility is located sufficiently inland away from the Pacific Ocean to be less subject to the strong land–sea circulation.

Note that the y-axis showing wind direction spans from 0 to 360 degrees in Figures B.2, B.5, and B.8. Comparing wind directions slightly above 0 degrees and below 360 degrees can be falsely interpreted as significant mismatches between observations and simulations. In fact, 0 and 360 degrees overlap and directions slightly above 0 degrees and below 360 degrees should be

---

[3] http://www.camx.com/download/support-software.aspx

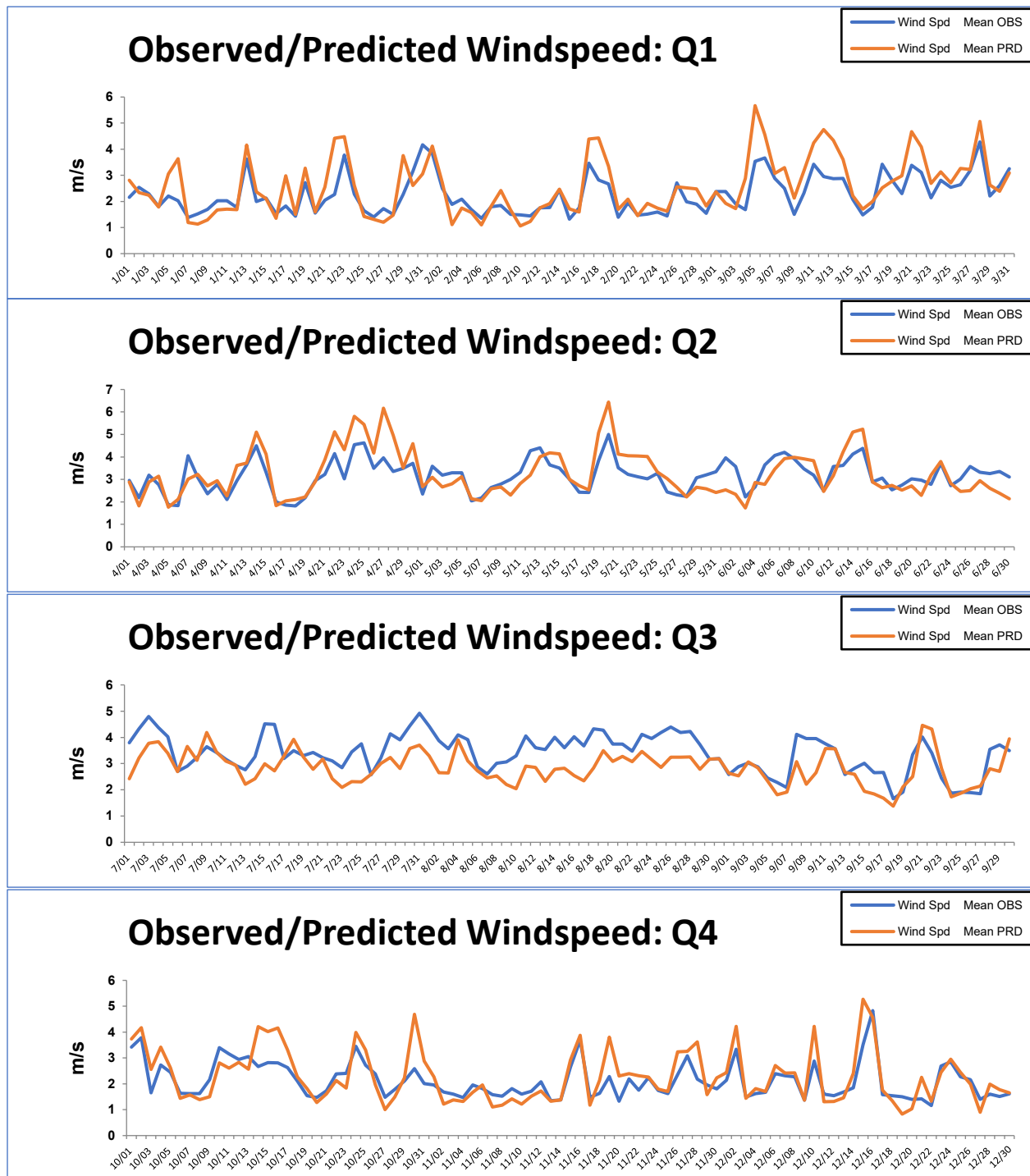interpreted as being in reasonably good agreement.

Figure B.1: Daily time series of observed and simulated wind speeds at the PBF East meteorological tower in Martinez for each quarter of 2016. "Mean OBS" is for all observations averaged over the 1-km domain. "Mean PRD" is for all prediction fields at the observation sites averaged over the 1-km domain.
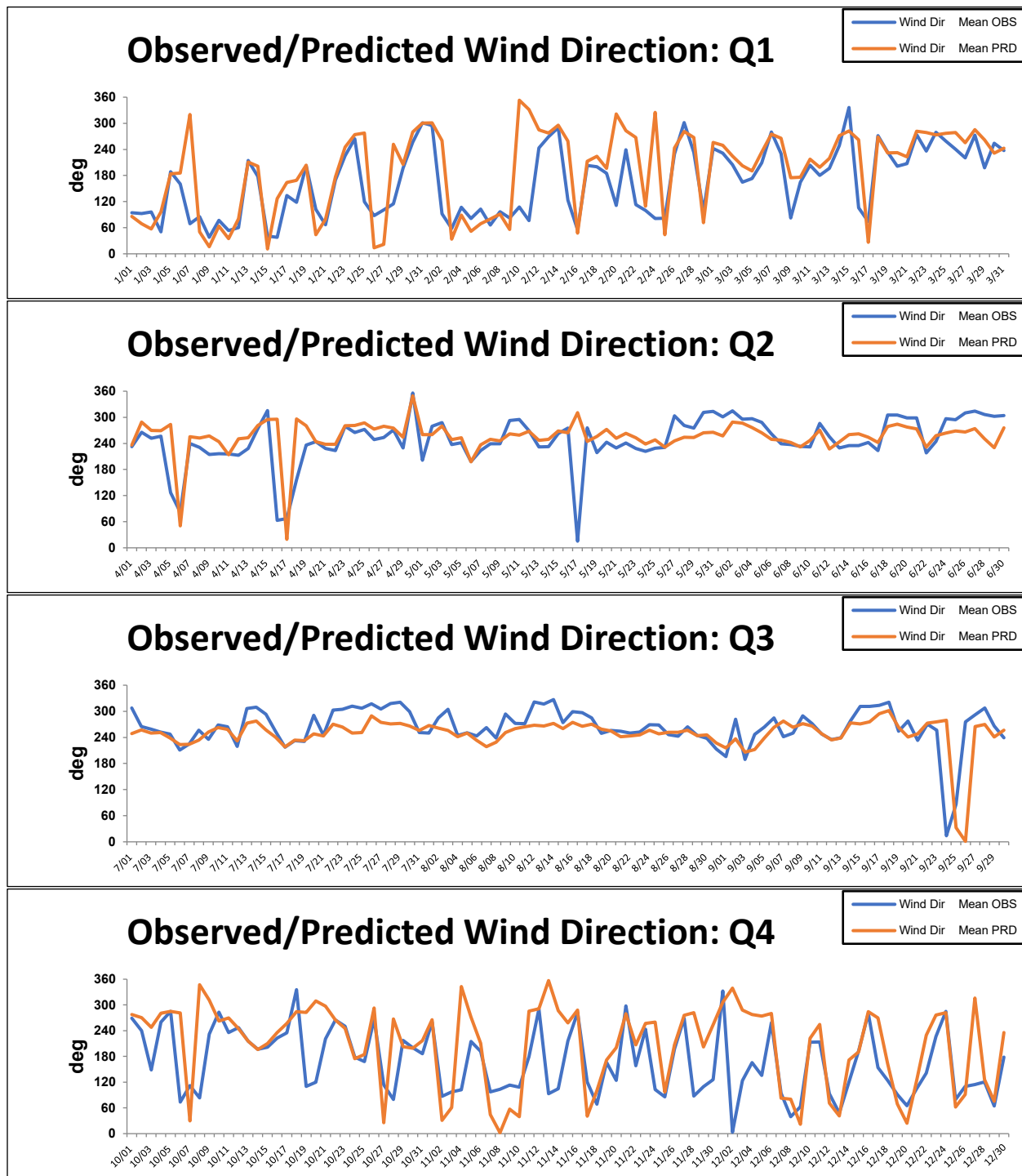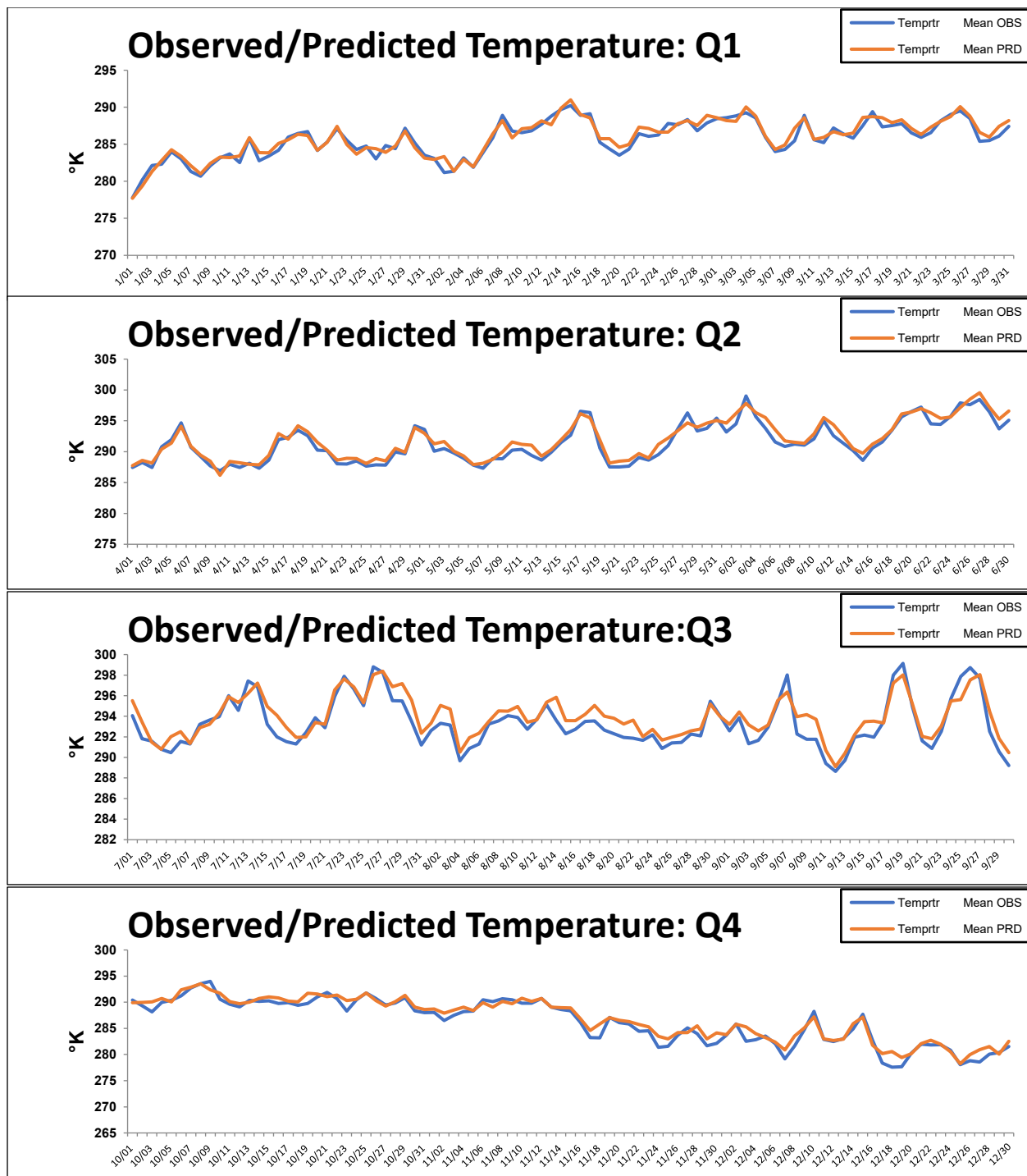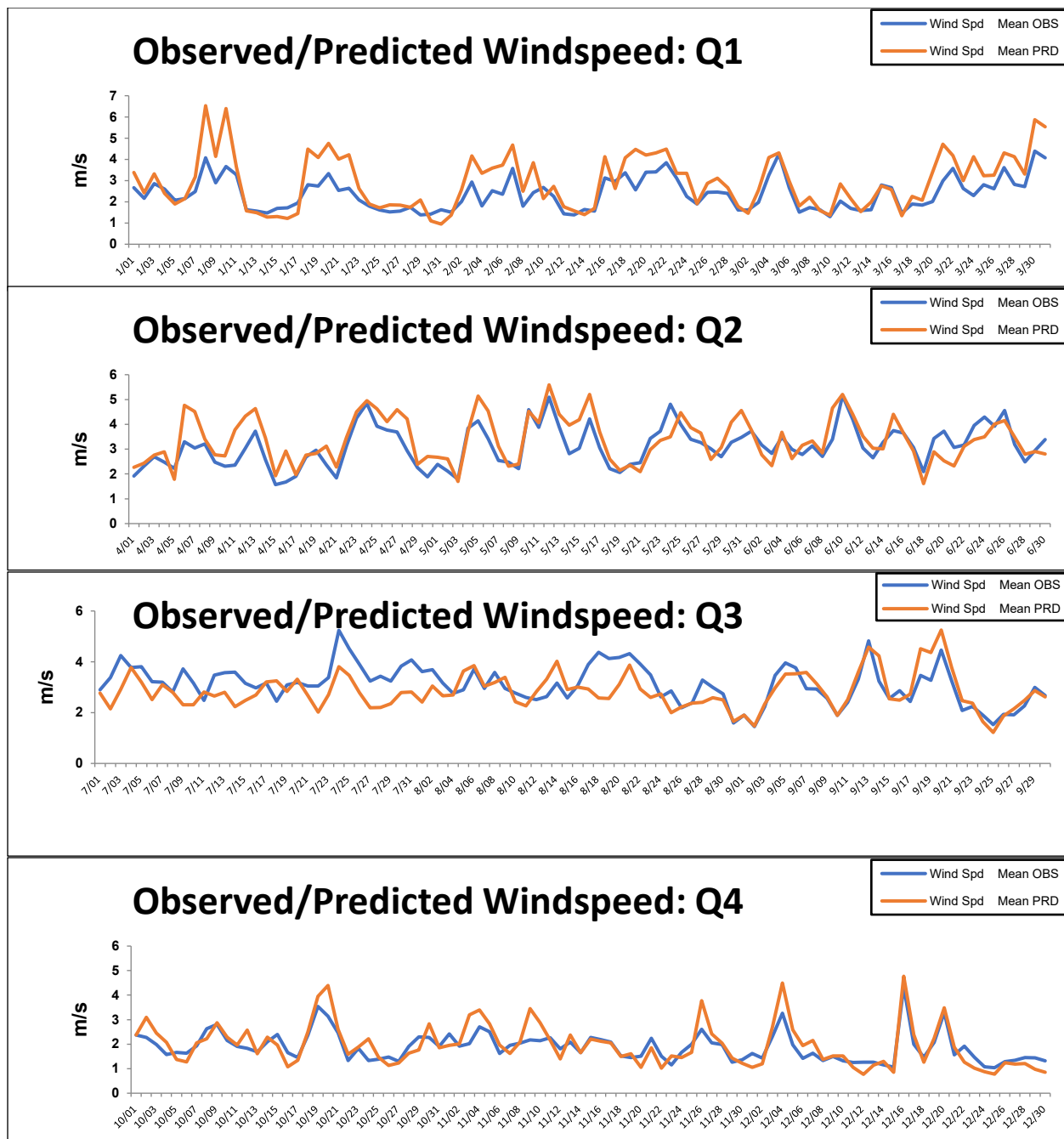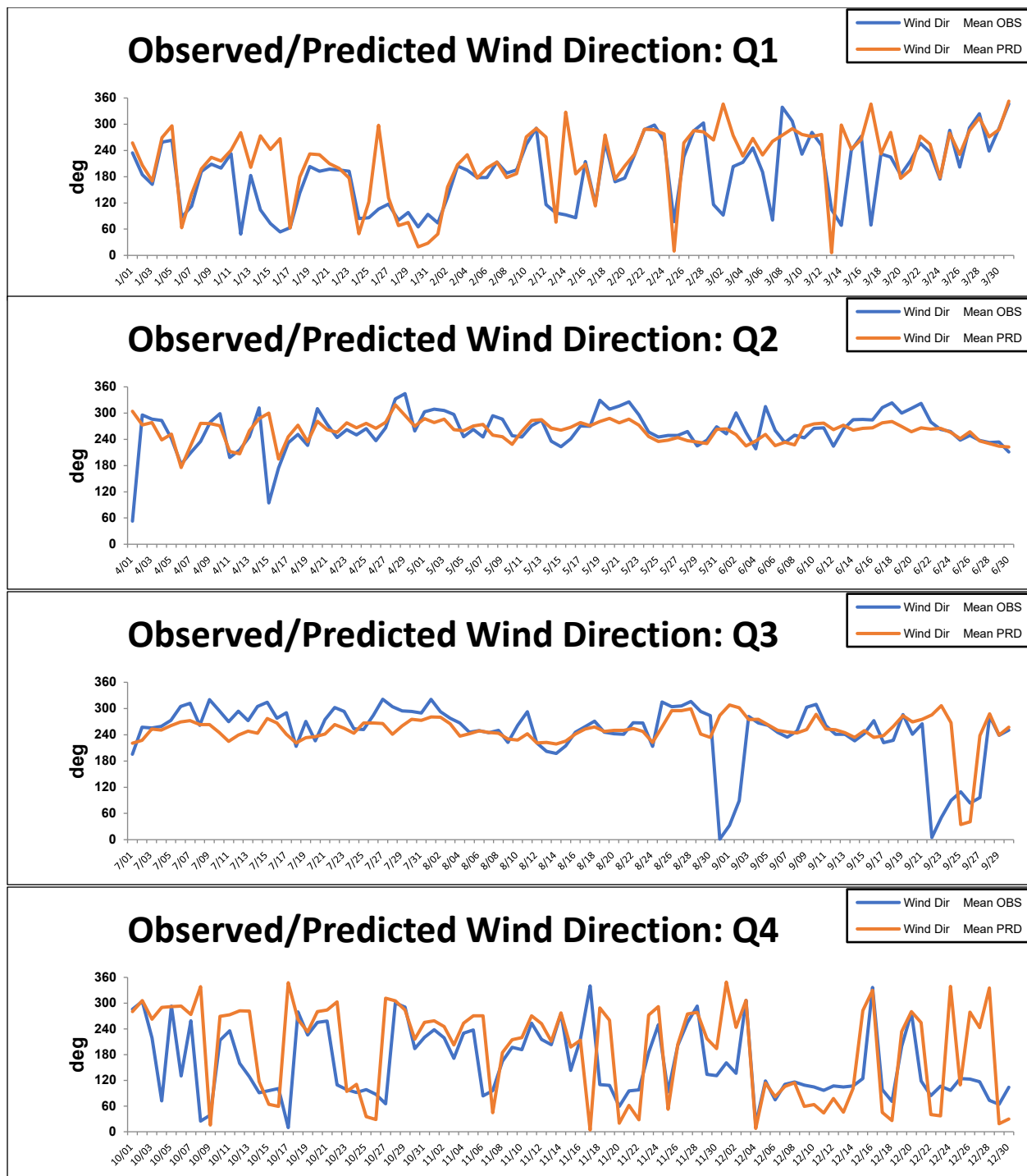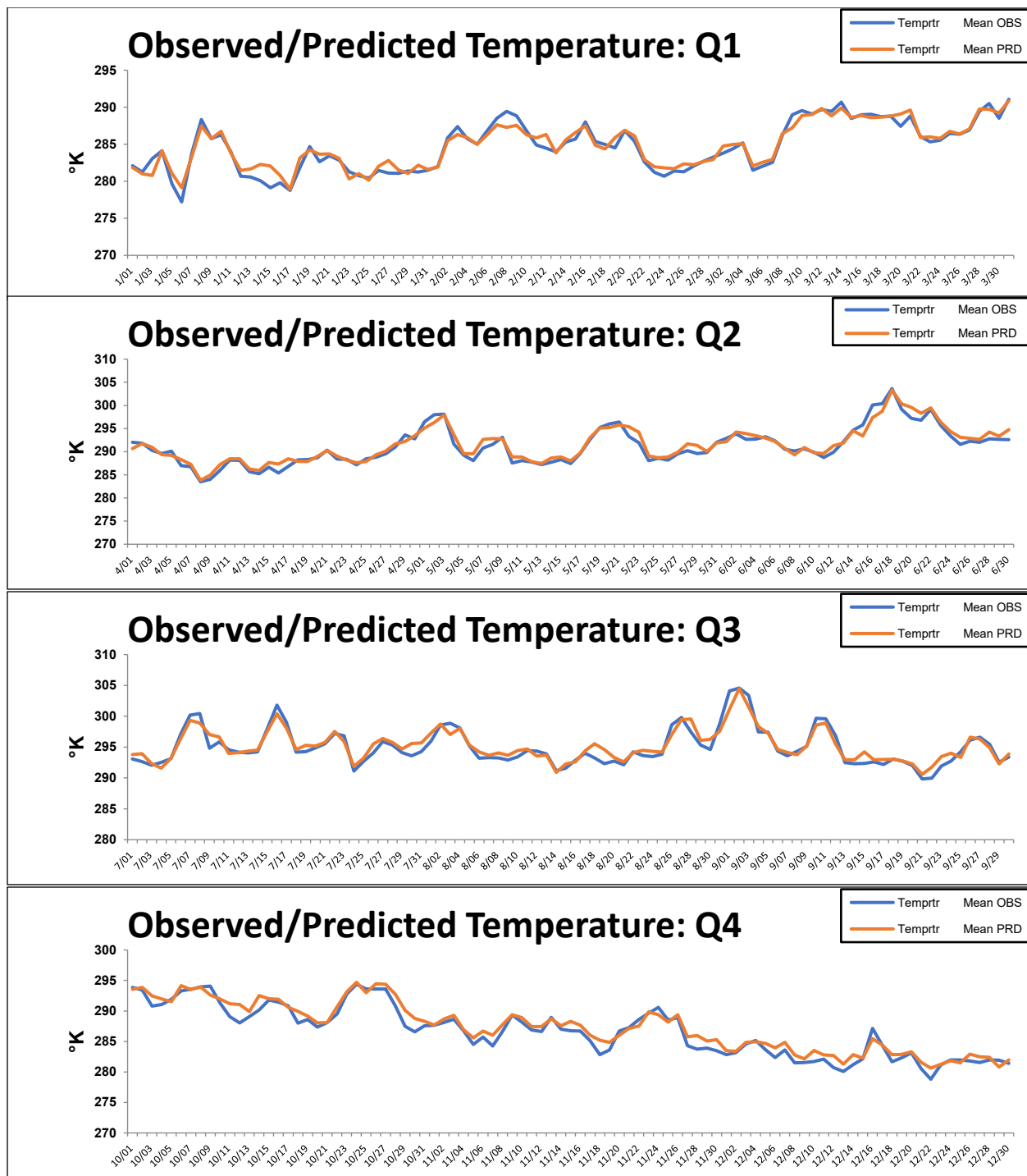
Figure B.2: Daily time series of observed and simulated wind directions at the PBF East meteorological tower in Martinez for each quarter of 2016. Note that 0 and 360 degrees overlap.

Figure B.3: Daily time series of observed and simulated temperatures at the PBF East meteorological tower in Martinez for each quarter of 2016.
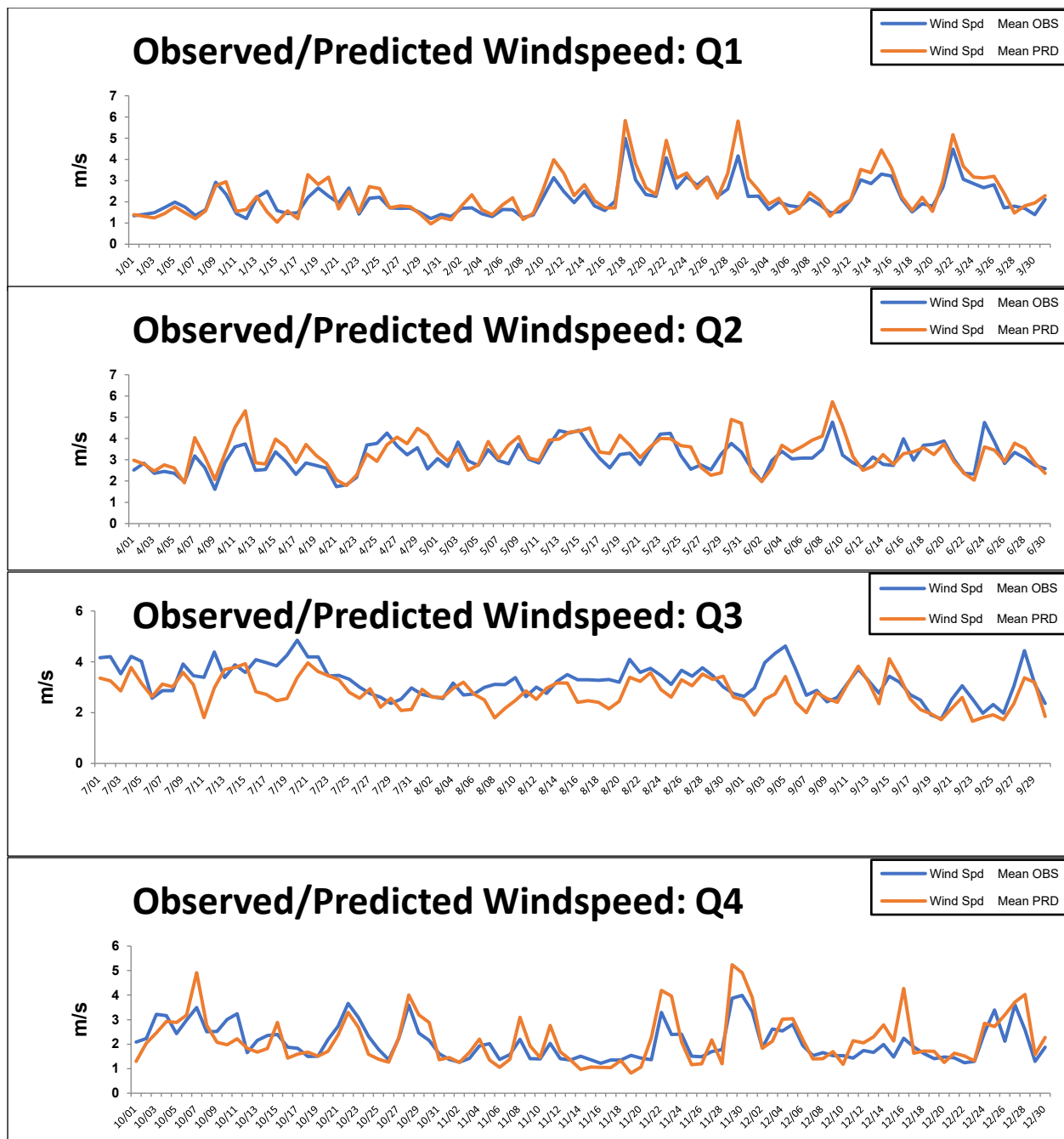
Figure B.4: Daily time series of observed and simulated wind speeds at the PBF East meteorological tower in Martinez for each quarter of 2017. "Mean OBS" is for all observations averaged over the 1-km domain. "Mean PRD" is for all prediction fields at the observation sites averaged over the 1-km domain.
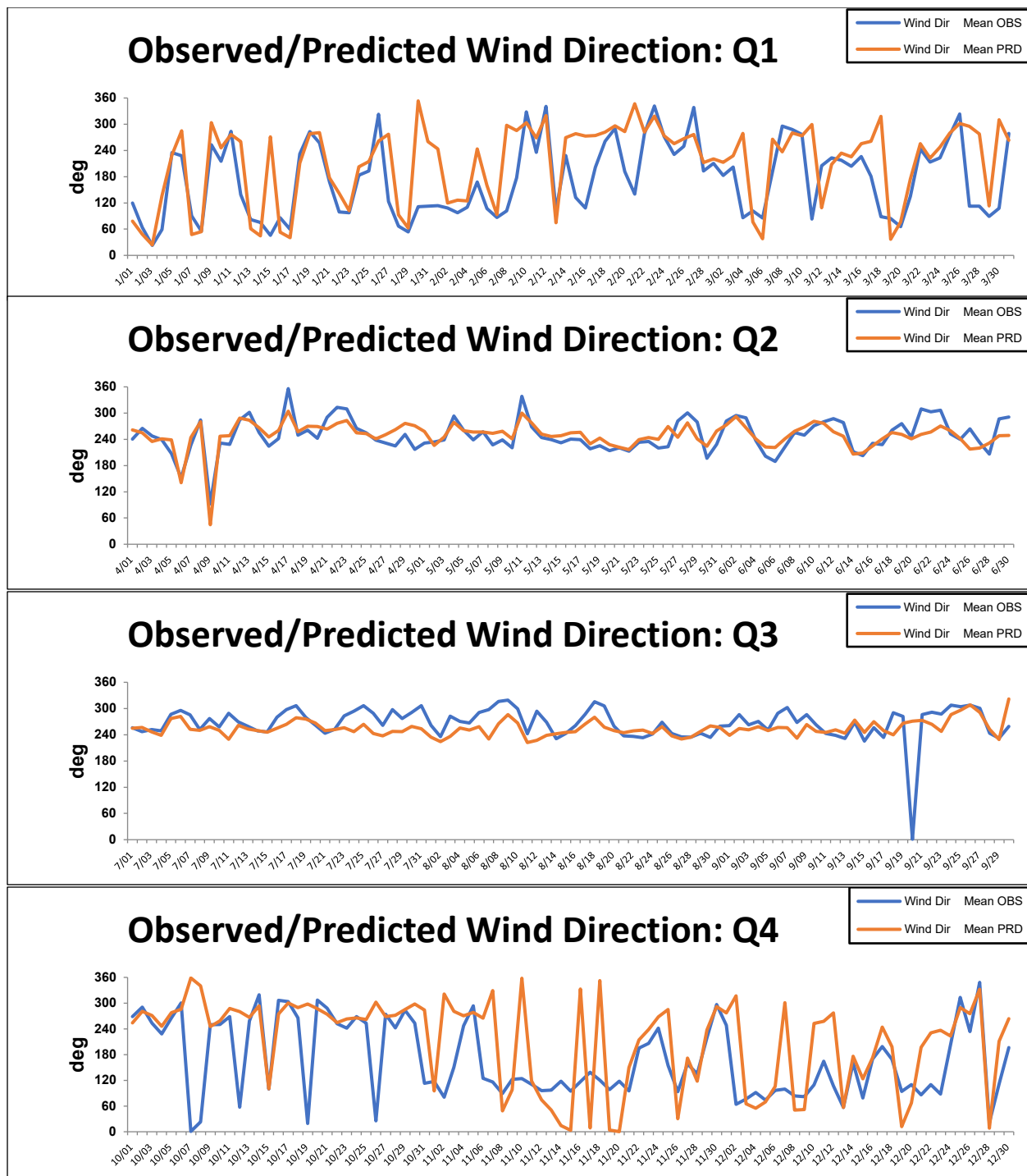
Figure B.5: Daily time series of observed and simulated wind directions at the PBF East meteorological tower in Martinez for each quarter of 2017. Note that 0 and 360 degrees overlap.
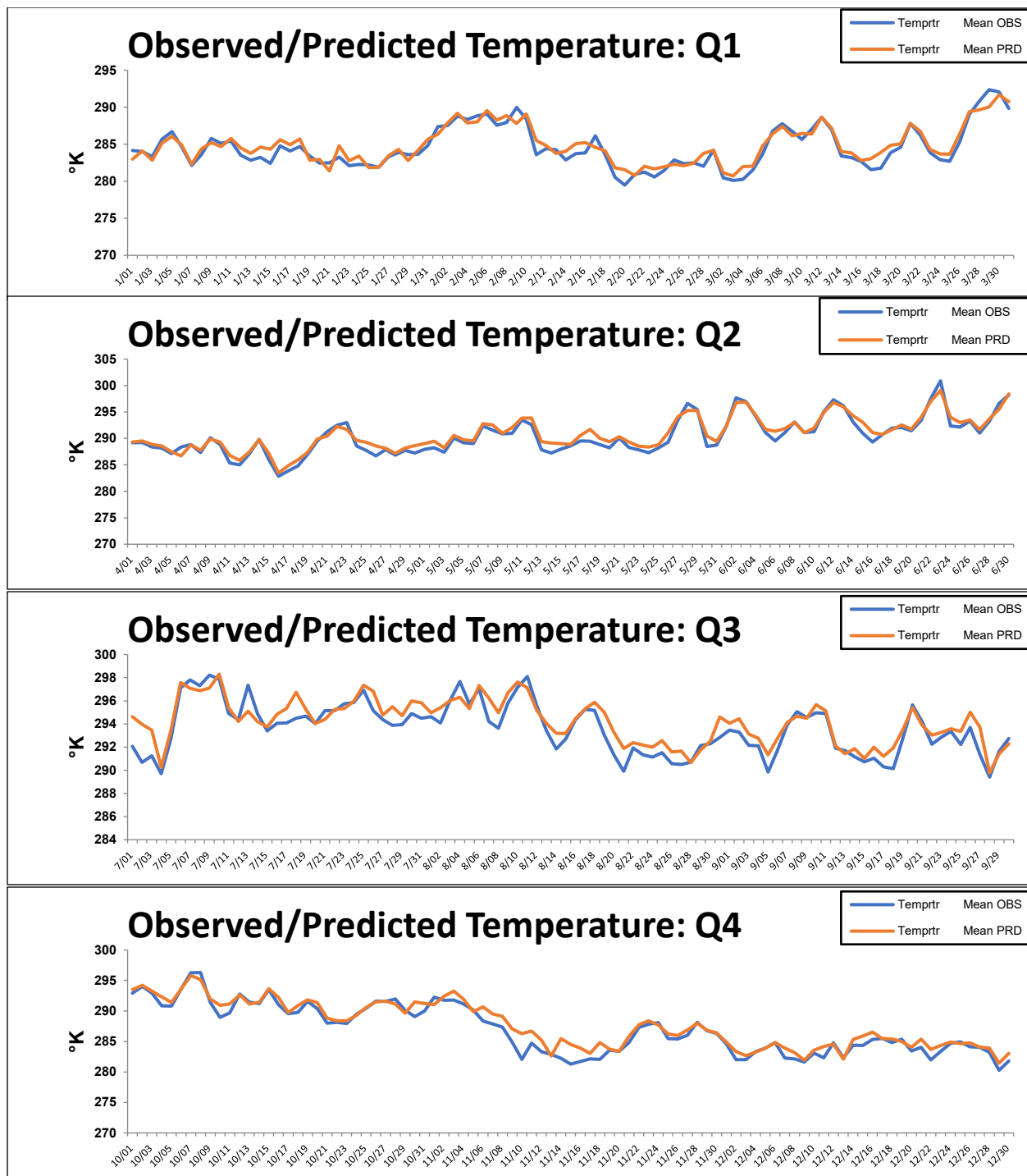
Figure B.6: Daily time series of observed and simulated temperatures at the PBF East meteorological tower in Martinez for each quarter of 2017.

Figure B.7: Daily time series of observed and simulated wind speeds at the PBF East meteorological tower in Martinez for each quarter of 2018. "Mean OBS" is for all observations averaged over the 1-km domain. "Mean PRD" is for all prediction fields at the observation sites averaged over the 1-km domain.

Figure B.8: Daily time series of observed and simulated wind directions at the PBF East meteorological tower in Martinez for each quarter of 2018. Note that 0 and 360 degrees overlap.

Figure B.9: Daily time series of observed and simulated temperatures at the PBF East meteorological tower in Martinez for each quarter of 2018.

B.2   Evaluating the WRF Model Against Upper Air Measurements

One upper air meteorological measurement station, located at Oakland International Airport and operated by the National Weather Service, is within the 1-km WRF modeling domain. Two daily measurements are conducted at 00 GMT and 12 GMT (4:00 pm and 4:00 am PST, respectively).

Outputs for the 1-km WRF model domain were compared against measurements at this site. For each day, simulations matched observations exceptionally well. Figures B.10 and B.11 show comparisons between simulations and observations for a winter and summer day for 2018. These days are randomly selected for the purpose of demonstration. They do not necessarily show the best or worst match between the simulations and observations.
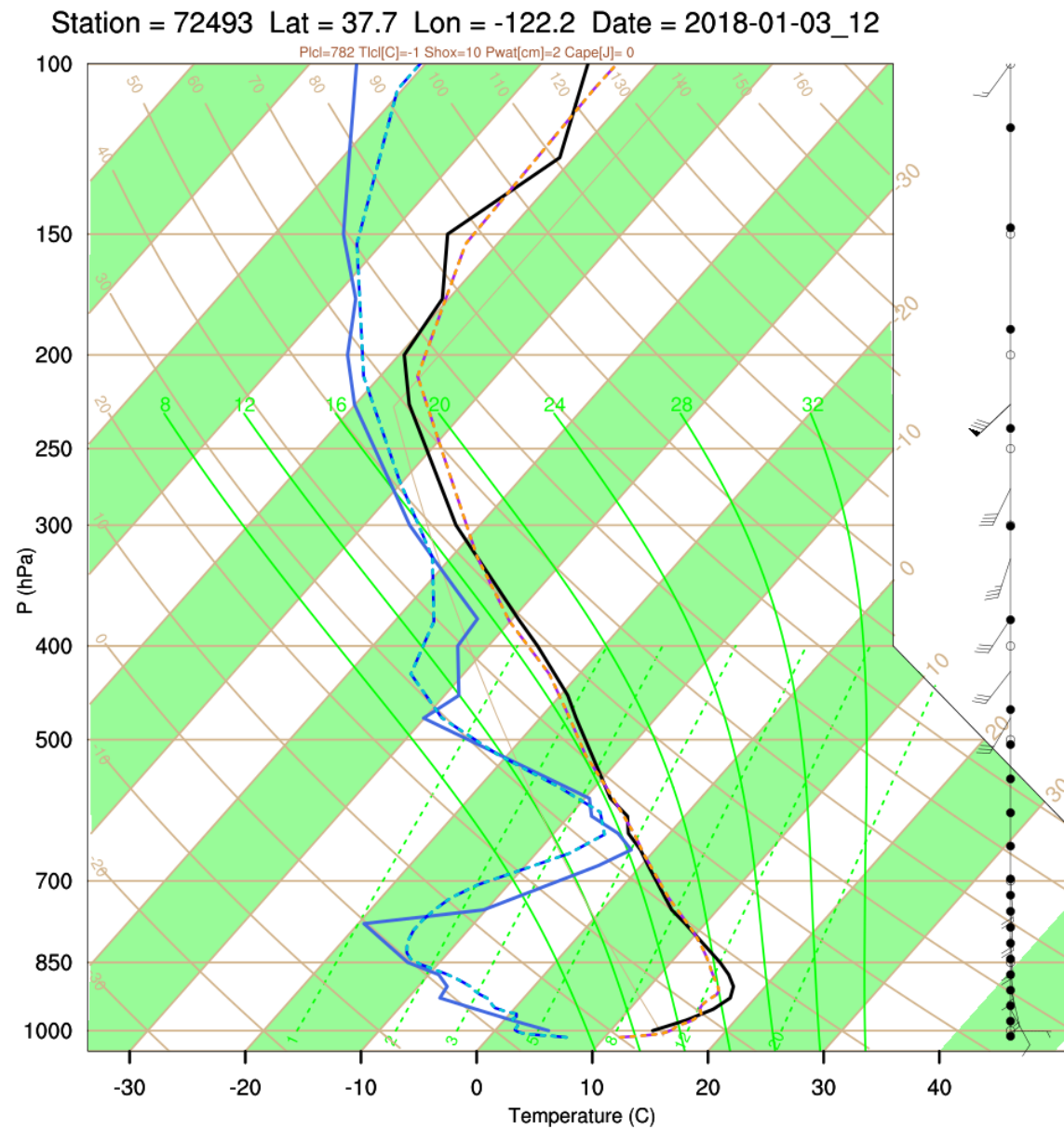
Figure B.10: A skew-T plot showing simulated (dashed lines) and observed (solid lines) temperatures (orange and black) and humidity (blue) at Oakland on January 3, 2018, at 12 GMT. Observed wind barbs at pressure levels are shown on the right y-axis.
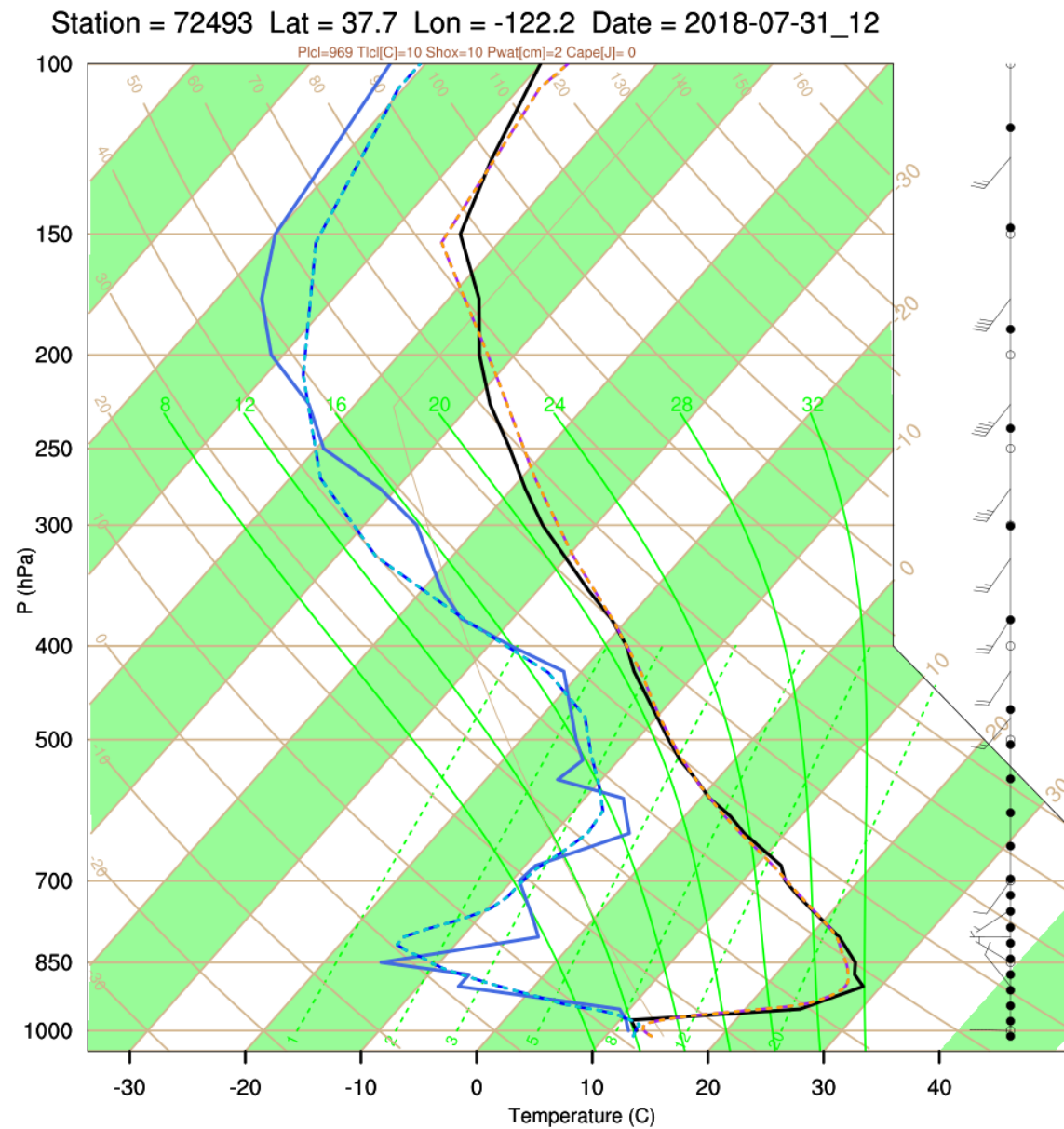
Figure B.11: A skew-T plot showing simulated (dashed lines) and observed (solid lines) temperatures (orange and black) and humidity (blue) at Oakland on July 31, 2018, at 12 GMT. Observed wind barbs at pressure levels are shown on the right y-axis.

Appendix C – CALPUFF Modeling Options

Primary PM$_{2.5}$ emitted from the PBF facility was modeled as an inert PM$_{2.5}$ species, i.e., secondary PM$_{2.5}$ formation in the atmosphere was not considered for this project. Pollutant removal processes due to wet scavenging and dry deposition were included. Parameters for wet scavenging and dry deposition are shown in Table C.1. Other CALPUFF modeling options used in this study are listed in Table C.2.

Table C.1: Parameters for wet scavenging and dry deposition.

Parameter		Value
Scavenging coefficient	Liquid precipitation	0.0001 s^{-1}
	Frozen precipitation	0.00003 s^{-1}
Particle size distribution	Geometric mean diameter	0.48 µm
	Geometric standard deviation	2.0 µm
Reference cuticle resistance		30 s/cm
Reference ground resistance		10 s/cm
Reference pollutant reactivity		8
# of particle-size intervals used to evaluate effective particle deposition velocity		9
Vegetation state in unirrigated areas		Active and unstressed vegetation

Table C.2: CALPUFF modeling technical options used in this study.

Option	Selected
Vertical distribution used in the near field	Gaussian
Terrain adjustment	Partial plume path adjustment
Subgrid-scale complex terrain	Not modeled
Near-field puffs modeled as elongated slugs	No
Transitional plume rise	Transitional rise computed
Stack tip downwash	Yes
Building downwash	No
Method used to compute plume rise for point sources not subject to building downwash	Briggs plume rise
Vertical wind shear modeled above stack top	No
Puff splitting	No
Gravitational settling (plume tilt)	No
Method used to compute dispersion coefficients	PG dispersion coefficients for rural areas; MP coefficients in urban areas
PG sigma (y, z) adjusted for roughness	No
Partial plume penetration of elevated inversion modeled for point sources	Yes
Strength of temperature inversion	Computed from measured/default gradients

Option	Selected
PDF used for dispersion under convective conditions	No
Subgrid TIBL module used for shoreline	No
Boundary conditions	No
Land use categories for which urban dispersion is assumed	13

Appendix D – CALPUFF Results

The purpose of this appendix is to provide additional information on CALPUFF results and to present findings from selected model performance evaluations. Since observations at air monitoring stations include PM$_{2.5}$ contributions from all sources (not just PBF), it is impossible to evaluate the model results against them. Therefore, we attempted to evaluate the model qualitatively, which includes examining the model's ability to capture monthly, seasonal, and year-to-year variability in concentration levels in response to changes in meteorological conditions.

Figure D.1 shows the annual average CALPUFF-simulated PM$_{2.5}$ concentrations for 2016, 2017, and 2018 across the 100-m receptor domain. There are some variations in concentrations among these years, which are thought to be due to year-to-year variability in meteorological conditions.

First, the areal extent of concentrations between 0.1 µg/m^3 and 0.5 µg/m^3 is different among these years. In 2016 and 2018, concentrations in this bin reached further to the east (covering Decker Island and Brannan Island State Recreation Area) compared with 2017, possibly due to stronger or more persistent westerly winds during those years.

In addition, monthly average PM$_{2.5}$ concentrations were calculated for each year, and the top five values within each month were then averaged to provide a representation of peak concentration levels. Differences in these top five monthly average concentrations were also evident among the three years, as shown in Figure D.2.

The model was able to capture differences among the same months across the years, as well as monthly variations within the same year. Differences among the same months across the years are significantly smaller than monthly variations within the same year. This is because vertical mixing is stronger during summer months, allowing more pollutants to reach ground level than in non-summer months.

Next, the number of receptors with annual average concentrations above 0.1 µg/m^3 was compared among the years, as shown in Table D.1. The number of receptors did not change significantly from year to year, indicating that while the shape of the emissions plume is different for each year due to year-specific meteorological conditions, the overall size of the area impacted does not change significantly.

Figure D.3 shows close-up maps of the 100-m receptor domain for 2016, 2017, and 2018. Areas covered by concentrations between 0.5 µg/m^3 and 1.0 µg/m^3 extend further in the northeast direction in 2016 and 2018 than in 2017. Conversely, the areas extend further in the southeast direction in 2017 than in 2016 and 2018. These close-up maps also show that year-to-year variability in concentrations is captured by the model.

For reference, we also plotted simulated annual average concentrations for 2016, 2017, and

2018 baseline emissions from only the FCCU for the 100-m receptor domain (Figure D.4) and for a close-up area of the 100-m domain (Figure D.5). Both sets of figures look reasonable.
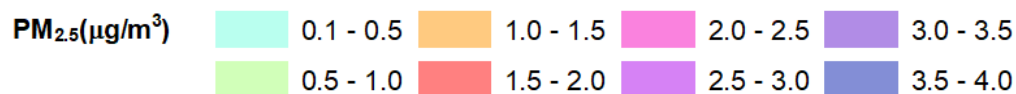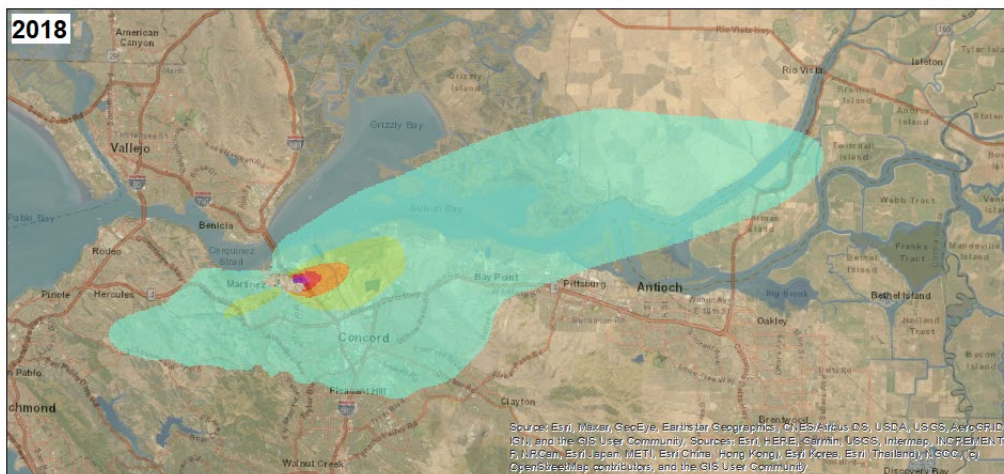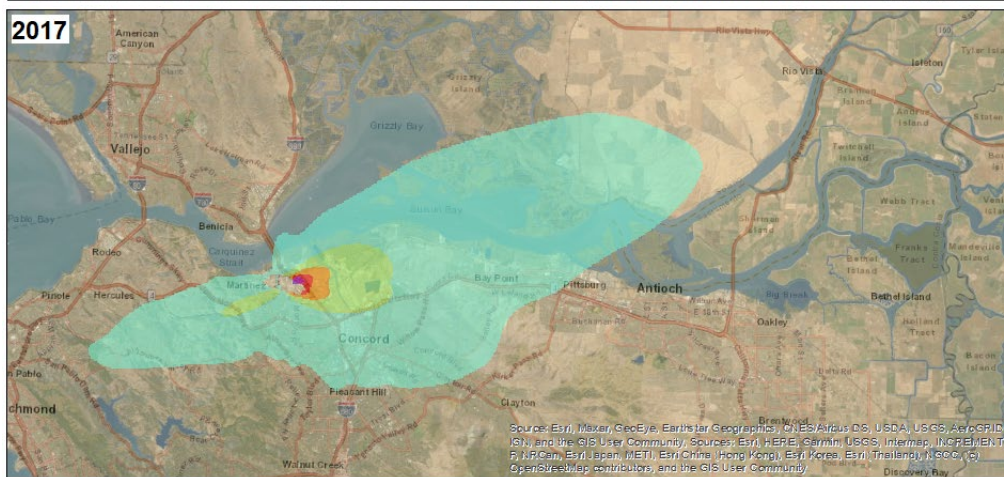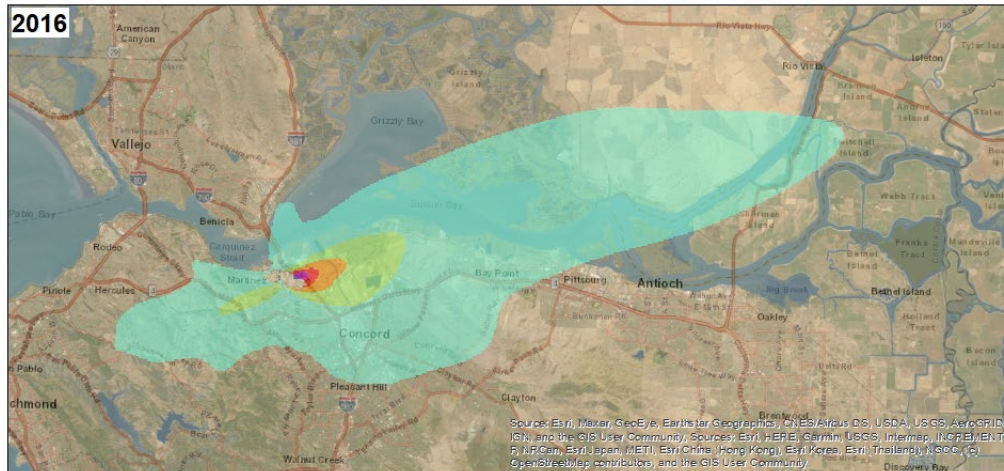
Figure D.1: Annual average CALPUFF-simulated PM$_{2.5}$ concentrations for the 100-m receptor domain for 2016, 2017, and 2018. PM$_{2.5}$ emissions from all PBF point sources were included in these simulations.
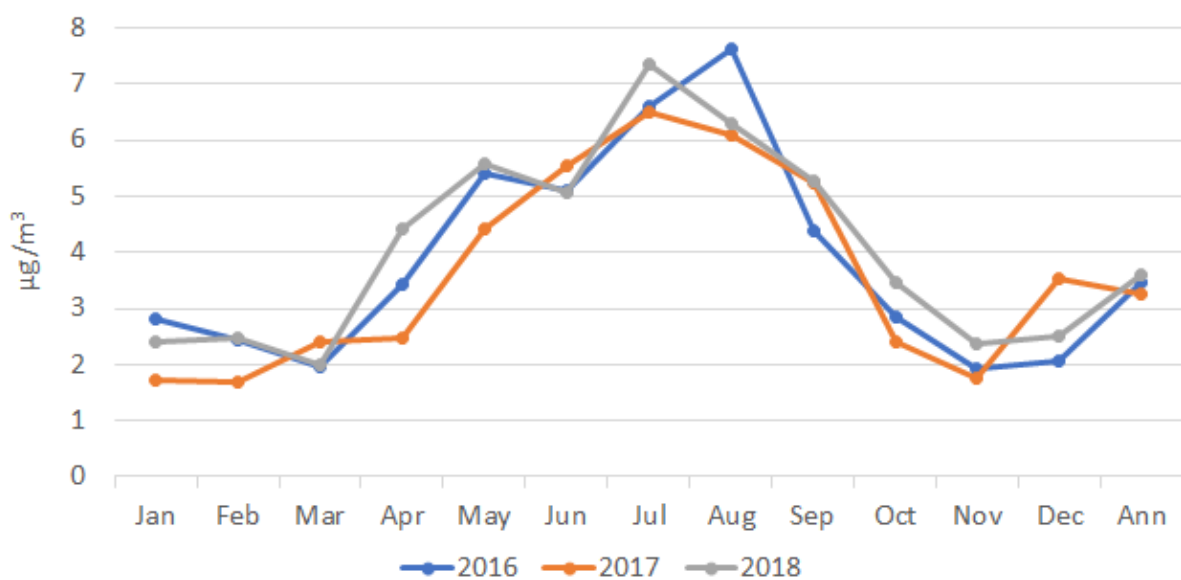
Figure D.2: Average of top five monthly average PM$_{2.5}$ concentrations for 2016, 2017, and 2018.

Table D.1: Number of 100-m receptors with CALPUFF-simulated annual average PM$_{2.5}$ concentrations above 0.1 µg/m³.

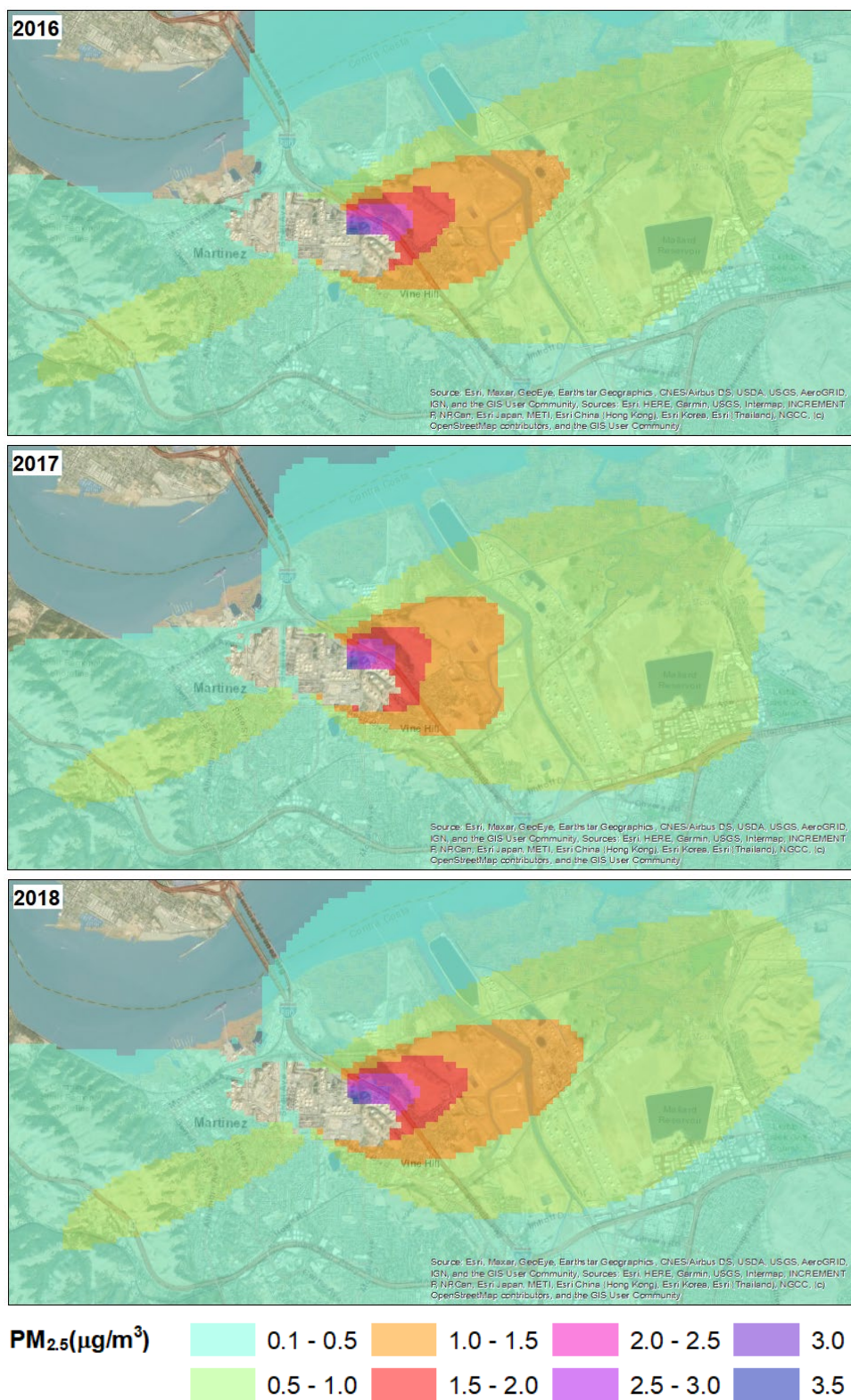| 2016	2017	2018
44,562	39,421	45,476

Figure D.3: Annual average CALPUFF-simulated PM$_{2.5}$ concentrations for 2016, 2017, and 2018 for a subset of the 100-m receptor domain that includes high-concentration areas. PM$_{2.5}$ emissions from all PBF point sources were included in these simulations.
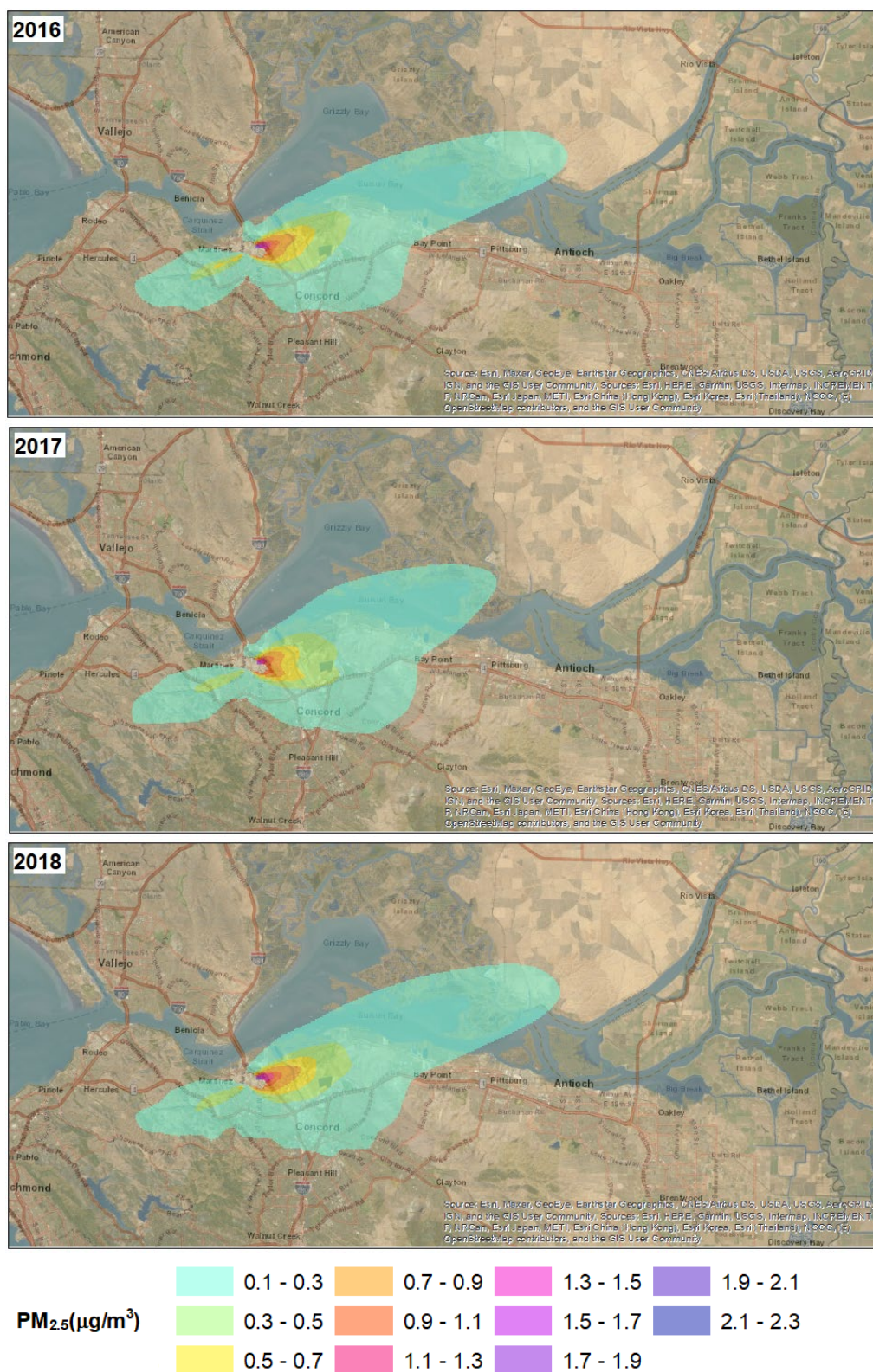
Figure D.4: Annual average CALPUFF-simulated PM$_{2.5}$ concentrations for the 100-m receptor domain for 2016, 2017, and 2018. PM$_{2.5}$ emissions from the FCCU only (without a WGS) were included in these simulations.
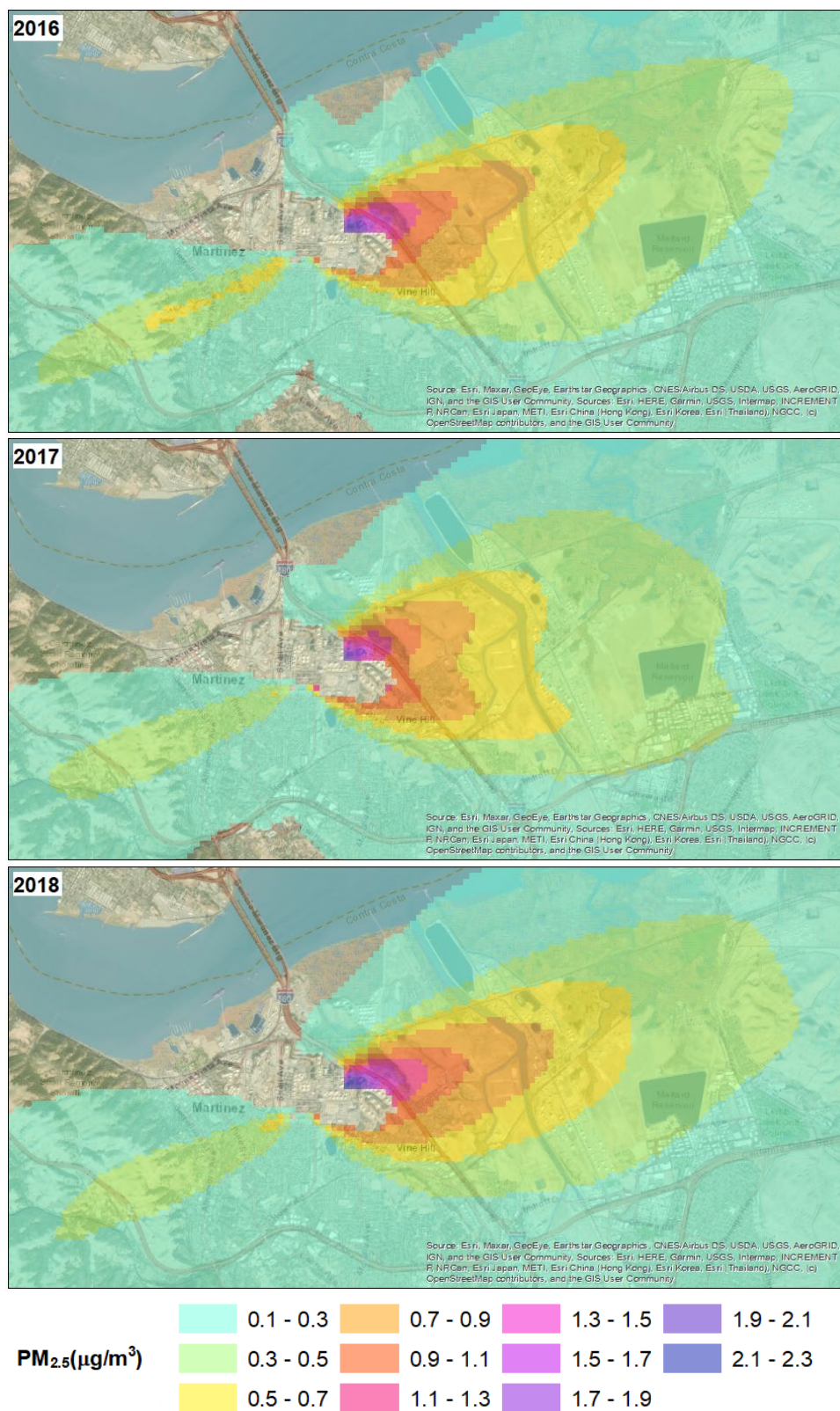
PM₂.₅(μg/m³)

0.1 - 0.3	0.7 - 0.9	1.3 - 1.5	1.9 - 2.1
0.3 - 0.5	0.9 - 1.1	1.5 - 1.7	2.1 - 2.3
0.5 - 0.7	1.1 - 1.3	1.7 - 1.9	

Figure D.5: Annual average CALPUFF-simulated PM₂.₅ concentrations for 2016, 2017, and 2018 for a subset of the 100-m receptor domain that includes high-concentration areas. PM₂.₅ emissions from the FCCU only (without a WGS) were included in these simulations.